

fuel fail in a fire, it is of interest for determining the source term to know if the fuel cladding is heated above its failure temperature (approximately 700°C to 800°C).

A modified version of the model for failure of a canister in a transportation cask was used to determine the probability that fuel will exceed this failure temperature. In the modified spreadsheet, the canister was replaced by the mass of fuel that would be heated during the fire. As in the bare canister analysis discussed in Section D2.1.4.1, this mass was estimated based on the calculated thermal penetration depth. Based on the information provided in the GA-9 SAR report (Ref. D4.1.34, p. 3.6-3), the following average spent fuel properties were determined: thermal conductivity = 1.5 W/m K, density × specific heat = 9.9×10^5 J/m³ K. For a 1-hour fire, the calculated thermal penetration depth is 7.4 cm and the effective fuel mass is 1,910 kg. Since the severe fires of greatest concern have durations of 1 hour or longer, this fuel mass represents a reasonable, but probably conservative, estimate.

Other modifications to the model included changes to model the geometry and materials used in the GA-4/GA-9 casks. The inputs to the model are presented in Table D2.1-9. As in the previous analyses, the model does not rely on neutron shield because it is liable to melt early in the transient.

The model was run for three different fuel failure temperatures: 700°C, 750°C, and 800°C. This range of failure temperatures represents the lower end of the values reported in the literature (Ref. D4.1.65, pp. 7-20 to 7-21). As shown in Table D2.1-10, the calculated fuel failure probabilities were less than 0.001.

Table D2.1-9. Model Inputs – Bare Fuel Cask

Model Parameter	Value	Basis/Rationale
Fuel Properties		
Heated Mass (kg)	1,910	Calculated based on thermal penetration depth (see text)
Specific Heat (J/kg K)	438	Average for fuel region taken from <i>Thermal Responses of TAD and 5-DHLW/DOE SNL Waste Packages to a Hypothetical Fire Accident</i> (Ref. D4.1.25, Table 15)
Effective Surface Area (m ²)	10.0	Projected area for radiation heat transfer. Calculated based on equivalent outer diameter of fuel region (0.66 m)
Emissivity	0.8	From <i>Thermal Responses of TAD and 5-DHLW/DOE SNL Waste Packages to a Hypothetical Fire Accident</i> (Ref. D4.1.25, Table 17)
Initial Temperature (K)	400	Estimated from fig 3.4-4 in GA-9 SAR (Ref. D4.1.34)
Transportation Cask Outer Shell		
Outer Diameter (m)	1.12	Equivalent diameter estimated based on GA-9 SAR (Ref. D4.1.34, Figure 1.2-9)
Wall Thickness (m)	0.0032	Minimum outer shell thickness listed in cask SAR (Ref. D4.1.34)
Length (m)	4.25	Length adjacent to the fuel region
Density (kg/m ³)	7850	Density of 516 carbon steel (Ref. D4.1.6, Section II, Part A, SA-20, 14.1)
Specific Heat (J/kg K)	604	Approximate value for 516 carbon steel at 400°C (Ref. D4.1.25, Table 10)

Table D2.1-9. Model Inputs – Bare Fuel Cask (Continued)

Model Parameter	Value	Basis/Rationale
Emissivity	0.8	Average value for carbon steel in Avallone and Baumeister, (Ref. D4.1.8, Table 4.3.2)
Initial Temperature (K)	344	Estimated from fig 3.4-4 in GA-9 SAR (Ref. D4.1.34)
Transportation Cask Gamma Shield^a		
Outer Diameter (m)	0.902	Equivalent diameter estimated based on GA-9 SAR (Ref. D4.1.34, Figure 1.2-9)
Wall Thickness (m)	0.107	Combined thickness of stainless steel and depleted uranium shields (steel: 0.0445 m; DU: 0.0622 m) (Ref. D4.1.34)
Length (m)	4.25	Length adjacent to the fuel region
Mass × Specific Heat (J/K)	3.45×10^6	Based on calculated masses of steel and DU and specific heats listed in GA-9 SAR (Ref. D4.1.34, Tables 2.2-1 and 3.2-2)
Emissivity	0.8	Average value for carbon steel in Avallone and Baumeister, (Ref. D4.1.8, Table 4.3.2)
Initial Temperature (K)	360	Estimated from fig 3.4-4 in GA-9 SAR (Ref. D4.1.34)
Post-Fire Conditions		
Ambient Temperature (K)	361	Post-fire temperature of 190°F from <i>Discipline Design Guide and Standards for Surface Facilities HVAC Systems</i> Ref. D4.1.16, Section 3.2). This value is 100 °F higher than the maximum interior facility temperature
Heat Transfer Coefficient (W/m ² K)	2.0	Natural convection based on anticipated post-fire surface temperature and standard convective heat transfer correlations (Results not sensitive to this value)

NOTE: ^a Composite properties representing both the stainless steel cask wall and depleted uranium gamma shield.

DU = depleted uranium; SAR = Safety Analysis Report.

Source: Original

Table D2.1-10. Summary of Fuel Failure Probabilities

Fuel Failure Temperature	Monte Carlo Results		Failure Probability	
	Total Failures	Total Trials	Mean	Standard Deviation
700°C	54	100,000	5.4×10^{-4}	7.4×10^{-5}
750°C	27	100,000	2.7×10^{-4}	5.2×10^{-5}
800°C	13	100,000	1.3×10^{-4}	3.6×10^{-6}

Source: Original

D2.1.5.4 Analysis To Determine Failure Probabilities For Casks Exposed To Fire

NUREG/CR-6672 (Ref. D4.1.65, Section 6) provides an analysis of seal failure in bare fuel transportation casks. The analysis uses a simple 1-D axisymmetric heat transfer model that is similar to the simple model used in the fire fragility analysis presented in Section D2. The simple model is used to determine the length of time the cask could be exposed to an 800°C or 1,000°C fire before seal failure would be predicted.

The report notes that the elastomer seals used in many transportation casks degrade completely at 500°C, but that the degradation rate increases significantly at 350°C (Ref. D4.1.65, p. 2-9). Other seal degradation information provided by cask vendors indicates that the maximum design temperature for the metallic o-ring seals in the TN-68 casks is 536°F (280°C) (Ref. D4.1.66, p. 3-2). This is the maximum safe temperature for continuous operation. The actual failure temperature for these seals would be much higher. Based on this information, seal failure is anticipated at temperatures of around 350°C to 450°C.

NUREG/CR-6672 indicates that the seals in a steel/depleted uranium truck cask would reach 350°C if exposed to a 1,000°C fire for 0.59 hours (Ref. D4.1.65, Table 6.5). In a steel/lead/steel (SLS) truck cask, this temperature would be reached in 1.04 hours. The times for rail casks were longer at 1.06 hours for an SLS rail cask and 1.37 hours for a monolithic steel rail cask.

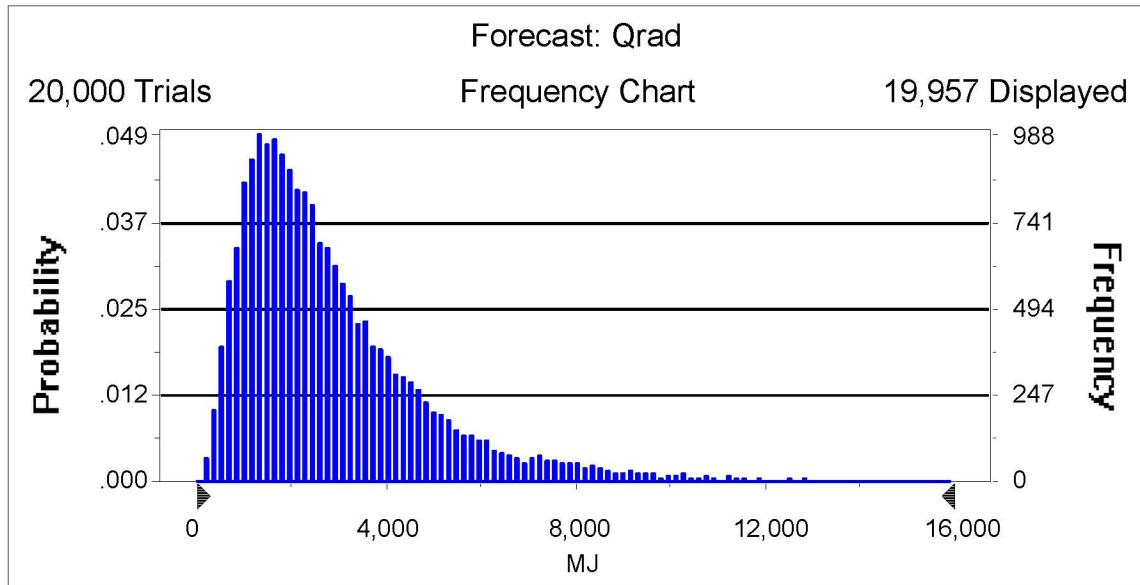
The probability distributions for fire temperature and fire duration discussed in section D2.1.1 can be used to determine the probability that the fire conditions listed in the preceding paragraph would be exceeded. This is accomplished by first determining the probability distribution (using Crystal Ball) for the maximum thermal radiation energy from the fire using the following equation:

$$Q_{\text{rad}} = \sigma A T_{\text{fire}}^4 t_{\text{fire}} \quad (\text{Eq. D-25})$$

where:

- σ = the Stefan-Boltzmann constant ($5.668 \times 10^{-8} \text{ W/m}^2 \text{ K}^4$)
- A = cask surface area exposed to the fire
- T_{fire} = fire temperature (sampled from the probability distribution)
- t_{fire} = fire duration (sampled from the probability distribution)

The probability distribution for Q_{rad} is shown in the figure below:



Source: Original

Figure D2.1-7. Distribution of Radiation Energy from Fire

Next, the value for Q_{rad} corresponding to the NUREG/CR-6672 fire temperature and duration for seal failure is calculated. The probability distribution for Q_{rad} can then be used to determine the probability that the fire will be severe enough to cause seal failure (i.e., will exceed the value for Q_{rad} calculated based on the NUREG/CR-6672 conditions).

The values for Q_{rad} corresponding to a 1,000°C fire and the fire durations reported in NUREG/CR-6672 are listed below along with the probability of exceedance determined from the probability distribution. The exceedance probabilities can be used as an estimate of the seal failure probability for seals that fail at the temperature, T_{fail} , listed in Table D2.1-11. For example, for a SLS truck cask that has seals that fail at 350°C, the probability that the seals fail due to a fire is 6.9×10^{-3} .

By multiplying the highest seal failure probability in Table D2.1-11 (0.05) by the highest probability of fire-induced cladding failure in Table D2.1-11 (5.4×10^{-4}), it is shown that the joint conditional probability of a fire that causes additional cladding failure in a truck cask, given a fire, is less than 3×10^{-5} . Because the fire initiating event frequency over the preclosure period of such truck cask fires is less than 1 (see Attachment F for the facilities that contain these, i.e., WHF and Intra-Site operations), such fires are beyond Category 2 and not analyzed further.

Table D2.1-11. Probabilities that Radiation Input Exceeds Failure Energy for Cask

Cask Type	T _{fail} (°C)	Temperature (°C)	Duration (hrs)	Q _{rad} (MJ)	P _{exceed}
Steel/DU Truck Cask	350	1,000	0.59	7,208	5.0 × 10 ⁻²
Steel/Lead/Steel Truck Cask	350	1,000	1.04	12,405	6.9 × 10 ⁻³
Steel/Lead/Steel Rail Cask	350	1,000	1.06	12,950	5.6 × 10 ⁻³
Monolithic Steel Rail Cask	350	1,000	1.37	16,737	1.7 × 10 ⁻³
Steel/DU Truck Cask	500	1,000	≈ 1.0 ^a	≈ 12,200	7.1 × 10 ⁻³
Steel/Lead/Steel Truck Cask	500	1,000	≈ 1.3 ^a	≈ 15,900	2.2 × 10 ⁻³

NOTE: ^a Estimated from Figure 6.6 in NUREG/CR-6672 (Ref. D4.1.65).

Source: Original

D2.2 SHIELDING DEGRADATION IN A FIRE

The NUREG/CR-6672 (Ref. D4.1.65) transportation study performed analyses on the internal temperatures of cask for long duration fires of 1,000°C. The transportation study included scenarios for fire-only and fire-plus-impact in the calculation of the probability of loss of shielding (LOS).

D2.2.1 Analysis of Loss of Shielding for Transportation Casks

All transportation casks contain separate gamma and neutron shields. The neutron shields are generally composed of a low melting point polymer material that would melt and offgas very quickly when exposed to a fire. For that reason, it is given that the neutron shield is always lost in fire scenarios. The composition of the gamma shield varies between cask designs, with some designs having layers of steel and depleted uranium, others having layers of steel and lead, or and others with layers of steel. Only casks containing lead could lose their gamma shielding in a fire.

As previously discussed, the thermal analyses for the transportation casks (Ref. D4.1.65, Table 6.5) shows that the internal regions of the cask reach the 350°C range in the range of 0.59 to 1.37 hours for the long duration 1,000°C fire. The least time represents the steel-depleted uranium casks and the longest the monolithic steel. The time to reach 350°C for SLS casks is about one hour. The time to reach the lead melting temperature (327.5°C) should be somewhat less than one hour but is not specified. However, NUREG/CR-6672 (Ref. D4.1.65) indicates that lead melting in itself does not result in significant LOS but the melting must be accompanied by outer shell puncture that permits the lead to flow out of the shield configuration.

NUREG/CR-6672 states that there are four characteristic fires of interest in the transportation risk analysis: 10 minutes as the duration of a typical automobile fire; 30 minutes for a regulatory fires; 60 minutes for an experimental pool fire for fuel from one tanker truck; and 400 minutes for an experimental pool fire from one rail tank car. These typical durations suggest that a real fire is unlikely to last long enough to result in a LOS condition for transportation scenarios.

D2.2.2 Probability of LOS in Fire Scenarios

Melting of the lead shielding and loss of containment of the molten lead results in loss of shielding for SLS casks. Two mechanisms for escape of the molten lead are considered:

- Puncture of the outer shell
- Rupture lead containment due to internal pressure

Puncture of the 2-inch thick (or more) outer shell, in addition to exposure to fire, would allow molten lead to escape, resulting in LOS. The shell puncture would be an independent failure with a probability of 10^{-8} for the low speeds at which the cask would be moving (Table 6.3-4). With the additional failure of exposure to fire, the LOS probability would be even less.

Containment of the molten lead could be lost due to thermal expansion of the lead coincident with the thermal weakening of the steel. Molten lead is cast into the cavity bounded by the inner and outer shells and the bottom plate ((Ref. D4.1.50, p. 1.1-4); (Ref. D4.1.49, p. 1.2-2); (Ref. D4.1.9, p. 1.2-5); and (Ref. D4.1.47, p. 1-5)). The lead contracts as it cools and solidifies. When the cask is exposed to a fire and the lead melts, it expands to reoccupy the volume when originally cast. When heated beyond the melting point, the liquid lead could continue to expand, exerting hoop stresses upon the inner and outer shells. The shells are thick and strong, e.g., the inner and outer shell thicknesses for the MP197 are 1.25 and 2.5 inches, respectively (Ref. D4.1.47, Drawing 1093-71-4, rev. 1), and the bottom plate thickness is 6.5 inches (Ref. D4.1.47, Drawing 1093-71-2, rev. 1). Consequently, failure of the steel is considered very unlikely.

As part of the PCSA, an attempt was made to analyze hydraulic failure of the molten lead containment due to a fire. Unfortunately, the thermal and physical properties of lead necessary for this analysis could not be found. Thus, hydraulic failure cannot be conclusively disproved. For that reason, a probability of 1.0 is used for LOS by transportation casks due to fire.

D2.2.3 Bases for Screening of Loss of Shielding Pivotal Events for Aging Overpacks in Fire Scenarios

This section summarizes the rationale for screening loss of shielding pivotal events associated with heating of aging overpacks in a fire. Loss of shielding could occur if the concrete that comprises the majority of the aging overpack spalled as a result of the fire. Spalling would reduce the thickness of the concrete and, if sufficient spalling occurs, the thickness could be reduced below the level required for adequate shielding.

D2.2.3.1 Thickness of Concrete Required for Adequate Shielding

The concrete thickness needed for adequate shielding can be estimated by determining the dose outside the overpack for different concrete thicknesses and comparing that dose to the exposure limits for radiation workers. For this calculation, the exposure rate on the surface of the aging overpack prior to the fire is 40 mrem/hr (Ref. D4.1.15, Section 33.2.4.17).

The dose outside the aging overpack is primarily due to Co-60 gamma radiation, the gamma attenuation due to concrete can be estimated based on data available from the National Institute

of Standards and Technology (NIST) (Ref. D4.1.40). This reference lists a value for the mass attenuation coefficient of the concrete divided by the concrete density (μ/ρ) of $0.058 \text{ cm}^2/\text{g}$ for the gammas produced by Co-60. Multiplying this value by an approximate concrete density of 2.3 g/cm^3 (Ref. D4.1.39, Table 4.2.5) yields a value for the mass attenuation coefficient of 0.133 cm^{-1} . Based on this value, there is approximately a factor of 10 reduction in the gamma dose for each 17.2 cm (6.8 inches) of concrete.

If the outer 6.8 inches of concrete were to spall as a result of the fire, the dose at the surface of the aging overpack would increase to 400 mrem/hr. If an additional 6.8 inches of concrete were to spall, the dose on the surface would be 4 rem/hr. The original concrete thickness is 34 inches based on existing aging overpack drawings (Ref. D4.1.14). There is 27.2 inches of concrete remaining after the first 6.8 inches of spallation and 20.4 inches of concrete remaining after the second 6.8 inches of spallation.

The dose outside the aging overpack can be estimated by noting that the dose decreases as the square of the distance from the source. After 13.6 inches of concrete has spalled, the dose 20.4 inches from the surface of the aging overpack would be 1 rem/hr, and the dose 61.2 inches from the surface would be 250 mrem/hr. Therefore, even in the case of extensive concrete spalling, workers involved in fire fighting or post-fire activities could be in close proximity to the degraded aging overpack for a lengthy period of time without exceeding either the annual exposure limit of 5 rem or special exposure limits outlined in 10 CFR Part 20 (Ref. D4.2.1, Paragraph 20.1206).

D2.2.3.2 Extent of Concrete Spalling in a Fire

The current aging overpack design has a steel liner outside the concrete shielding. Consequently, spalling and removal of concrete from the surface cannot occur unless the steel liner is removed or fails catastrophically. However, because alternative aging overpack designs have been considered without a steel outer liner, the potential for substantial spallation with a bare concrete shield was assessed.

Extensive spalling of structural concrete has been observed under some conditions when the structural concrete is exposed to intense fires. The most extensive spalling has been observed in tunnel fires, such as the Channel Tunnel fire in 1996. In such cases, a significant fraction of the concrete spalled when exposed to the intense heat from the long-duration fires.

Due to the potential significance of spalling in reducing the strength of concrete support structures, spallation of concrete has been the subject of considerable study. "Limits of Spalling of Fire-Exposed Concrete." (Ref. D4.1.37) provides a good overview of the factors that control concrete spalling due to fire. Hertz indicates that there are three types of spalling that can occur: (1) aggregate spalling, (2) explosive spalling, and (3) corner spalling. Aggregate spalling occurs with some aggregates (such as flint or sandstone) and results in superficial craters on the surface of the concrete. Corner spalling occurs only on the convex corners of beams or other structures and is caused by a localized weakening and cracking of the concrete such that the corner breaks off under its own weight. This mode of spalling is not relevant for the aging overpacks. Explosive spalling occurs when sufficient pressure builds up inside the concrete to cause pieces of concrete to be ejected from the surface. Explosive spalling is believed to account

for the extensive concrete loss observed in the Channel Tunnel fire. Of the three modes of spalling, only explosive spalling could produce the loss of concrete necessary to significantly reduce the shielding capability of the aging overpack.

“Predicting the fire resistance behaviour of high strength concrete columns,” (Ref. D4.1.43) notes that explosive spalling occurs when sufficient pressure builds up in the pores of the concrete to cause ejection of concrete from the surface. Buildup of such a high pressure requires three things: (1) low concrete permeability, (2) high moisture content in the concrete, and (3) rapid heating and resulting large thermal gradients. In addition, “Limits of Spalling of Fire-Exposed Concrete.” (Ref. D4.1.37) notes that spallation is more pronounced in concrete structures undergoing high compressive stress, such as support columns.

Low permeability prevents gas migration and allows pressure to build. High structural strength concretes, such as those used in tunnel construction, are known to have very low permeability and are therefore more prone to spalling. In contrast, normal strength concretes do not have low permeability and spallation is not observed (Ref. D4.1.43). Because the concrete used for shielding in the aging overpacks is not counted on for structural strength and is therefore classified as normal strength concrete², spallation is unlikely to occur.

Moisture content is a major factor in pressure buildup because water vapor is the gas primarily responsible for high pore pressures in the concrete. The concrete in the aging overpacks is unlikely to have a high moisture content because it is heated both internally by decay heat and externally by solar heat. In addition, it is likely to have been sitting in the Nevada desert for a lengthy period of time.

Thus, although the fire will produce large thermal gradients in the concrete, these gradients are unlikely to result in pressure buildup sufficient to cause extensive spallation due to the expected high permeability and low moisture content of the aging overpack concrete. This would be true regardless of whether the outer steel liner is present or not.

D2.2.3.3 Conclusion

The preceding discussion has shown that a substantial amount of concrete would have to spall during a fire to produce a hazard to workers involved in either fire fighting or post-fire activities. In addition, it was shown that spallation is very unlikely given the type of concrete to be used in the aging overpacks and the likelihood that the aging overpacks will have an outer steel liner. For these reasons, loss of aging overpack shielding in a fire is considered Beyond Category 2 and need not be analyzed further.

D3 SHIELDING DEGRADATION DUE TO IMPACTS

Neutrons emitted from transportation casks are shielded by a resin surrounded by a steel layer. The neutron shielding is present in the top lid, bottom, and shell. Neutron shields designed to 10 CFR Part 71 (Ref. D4.2.2) are robust against 10 CFR Part 71 hypothetical accident conditions

² For example, the compressive strength of the concrete used in the HI-STORM storage overpack (Ref. D4.1.39, Table 1.D.1) is listed as 3,300 psi or 22.75 MPa, which is well below the strength of 55 MPa usually defined as necessary for high strength concrete (Ref. D4.1.43).

related to impacts or drops, exhibiting factors of safety greater than 1 for Service Level D allowables. Meeting *2004 ASME Boiler and Pressure Vessel Code* Service Level D (Subsection NF) (Ref. D4.1.6) provides for twice the allowable stress intensity as normal operation but still results in an extremely low failure probability. In addition, neutron dose typically attenuates quickly with distance from the transportation cask so it is only a small fraction of the gamma dose to personnel more than two meters away. Evacuation to that distance is the way to reduce personnel dose from neutrons. For these reasons, the analysis below focuses on the principal threat to workers on the site, which is degradation of gamma shielding.

This section summarizes information on loss of shielding mechanisms that could occur in event sequences for repository waste handling operations. The information is derived from transportation cask accident risk analyses. This information provides insights and bases for estimating probabilities of passive failures that result in LOS for casks and overpacks in waste handling event sequences.

The repository facilities process three categories of waste containers that provide shielding: transportation casks (truck and rail) and aging overpacks. The event sequence diagrams for operations involving processing of transportation casks and aging overpacks include the pivotal event “loss of shielding” for event sequences that are initiated by physical impact or fire. LOS due to fire was addressed previously in section D2.2 of this attachment. The following discussion focuses specifically on LOS due to drops and impacts.

The information in this section is based in large part on results of FEA performed for four generic transportation cask types for transportation accidents as reported in NUREG/CR-6672 (Ref. D4.1.65) and NUREG/CR-4829 (Ref. D4.1.32). The results of the FEA were used to estimate threshold drop heights and thermal conditions at which LOS may occur in repository event sequences, using damage severity levels keyed to the FEA results to determine the challenge needed to cause LOS. The four cask types included one steel monolith rail cask, one steel/depleted uranium truck cask, one SLS truck cask and one SLS rail cask. NUREG/CR-6672 states that the steel in any of the cask is thick enough to provide some shielding, but the depleted uranium and lead provide the primary gamma shielding for the multi-shell cask types. The referenced study performed structural and thermal analyses for both failure of containment boundaries and loss of shielding for accident scenarios involving rail cask and truck cask impacting unyielding targets at impact speeds of 30-60, 60-90, 90-120, and greater than 120 mph. The impact orientations included side (0–20 degrees), corner (20 degrees–85 degrees), and end (85 degrees–90 degrees). The referenced study also correlated the damage from impacts on real targets including soil and concrete.

The event sequences used in the transportation accident analyses included impact-only, impact plus-fire, and fire-only conditions. The results of the FEA indicate that LOS could occur in the impact-only at speeds as low as 30 mph with an unyielding target and in fire scenarios of sufficient intensity and duration. The structural analyses did not credit the energy absorption capability of impact limiters. Therefore, the results are deemed applicable to approximate the structural response of transportation and similar casks in drop scenarios.

The primary reference NUREG/CR-6672 (Ref. D4.1.65), however, does not provide a threshold below which no LOS could be assured. Therefore, information quoted in an evaluation by the

Association of American Railroads (AAR) (Ref. D4.1.30) was used to establish thresholds for LOS conditions based on damage categories that are correlated to plastic strain in the inner shell of a cask. That information is based on a prior transportation accident analysis known as the Modal Study (Ref. D4.1.32). For potential PCSA applications, FEA results for inner shell strain versus impact speed were extended to estimate the lower bound of impact speed or drop heights to establish conditions at which LOS may occur in cask-drop scenarios in repository operations.

NUREG/CR-6672 (Ref. D4.1.65) addresses two modes of LOS in accident scenarios: deformations of lid and closure geometry that permit direct streaming of radiation; and/or reductions in cask wall thickness or relocation of the depleted uranium or lead shielding. The LOS due to lid/closure distortion can be accompanied by air-borne releases if the inner shell of the cask is also breached.

The results of the FEA reported in NUREG/CR-6672 (Ref. D4.1.65) provide some definitive results that are deemed to be directly applicable to the repository event sequence analyses:

- Monolithic steel rail casks do not exhibit any LOS, but there may be some radiation streaming through gaps in closure in any of the impact scenarios. This result can be applied to both transportation casks.
- Steel/depleted uranium/steel truck cask exhibited no LOS, explained by modeling that included no gaps between forged depleted uranium segments so that no displacement of depleted uranium could occur.
- The SLS rail and truck casks exhibit LOS due to lead slumping. Lead slump occurs mostly on end-on impact with a lesser amount in corner orientation. For side-on orientation, there is no significant reduction in shielding.

Therefore, this analysis focuses on LOS for SLS casks to estimate the drop or collision conditions that could result in LOS from lead slumping. Figure D3.2-1 illustrates the effect of cask deformation and lead slumping for a SLS rail cask following an end-on impact at 120 mph onto an unyielding target from the result of the FEA reported in NUREG/CR-6672 (Ref. D4.1.65).

D3.1 DAMAGE THRESHOLDS FOR LOS

The AAR study (Ref. D4.1.30) is used as a reference for this report. The information cited, however, was derived from an earlier transportation cask study known as the “Modal Study,” (Ref. D4.1.32). The Modal Study assigned three levels of cask response characterized by the maximum effective plastic strain within the inner shell of a transport cask. The severity levels are defined as:

- S1—implies strain levels < 0.2%
- S2—implies strains between 0.2 and 2.0%
- S3—implies strain levels between 2.0 and 30%.

The amount of damage to a cask for the respective severity levels is summarized in the following:

S1:

- No permanent dimensional change
- Seal and bolts remain functional
- Little if any radiation release
- Less than 40-g axial force on lead for all orientations
- No lead slump
- Fuel basket functional; up to 3% of fuel rods may release into cask cavity
- Loads/releases within regulatory criteria.

S2:

- Small permanent dimensional changes
- Closure and seal damage; may result in release
- Limited lead slump
- Up to 10% of fuel rods release to cask cavity.

S3:

- Large distortions
- Seal leakage likely
- Lead slump likely
- 100% fuel rods release to cask cavity.

As stated above, limited lead slumping may occur at damage level S2, but is likely to occur at damage level S3. The respective strain levels associated with damage levels S2 and S3 were applied to the results from NUREG/CR-6672 (Ref. D4.1.65) to establish a threshold impact speed for the onset of LOS.

D3.2 SEVERITY OF DAMAGE VERSUS IMPACT VELOCITY

The FEA results given in Table 5.3 of NUREG/CR-6672 (Ref. D4.1.65) are summarized in Table D3.2-1. The strain in the inner shell of the SLS casks are shown in Table D3.2-1 and illustrated in Figure D3.2-1. These data were plotted (Figures D3.2-2 and D3.2-3). The data points start at the lowest speed range of 30 to 60 mph. The data were plotted as points using the lower boundary of each of the four speed ranges on the abscissa. The strain plots were extended to the origin by including the point (0, 0) with the Table D3.2-1 data.

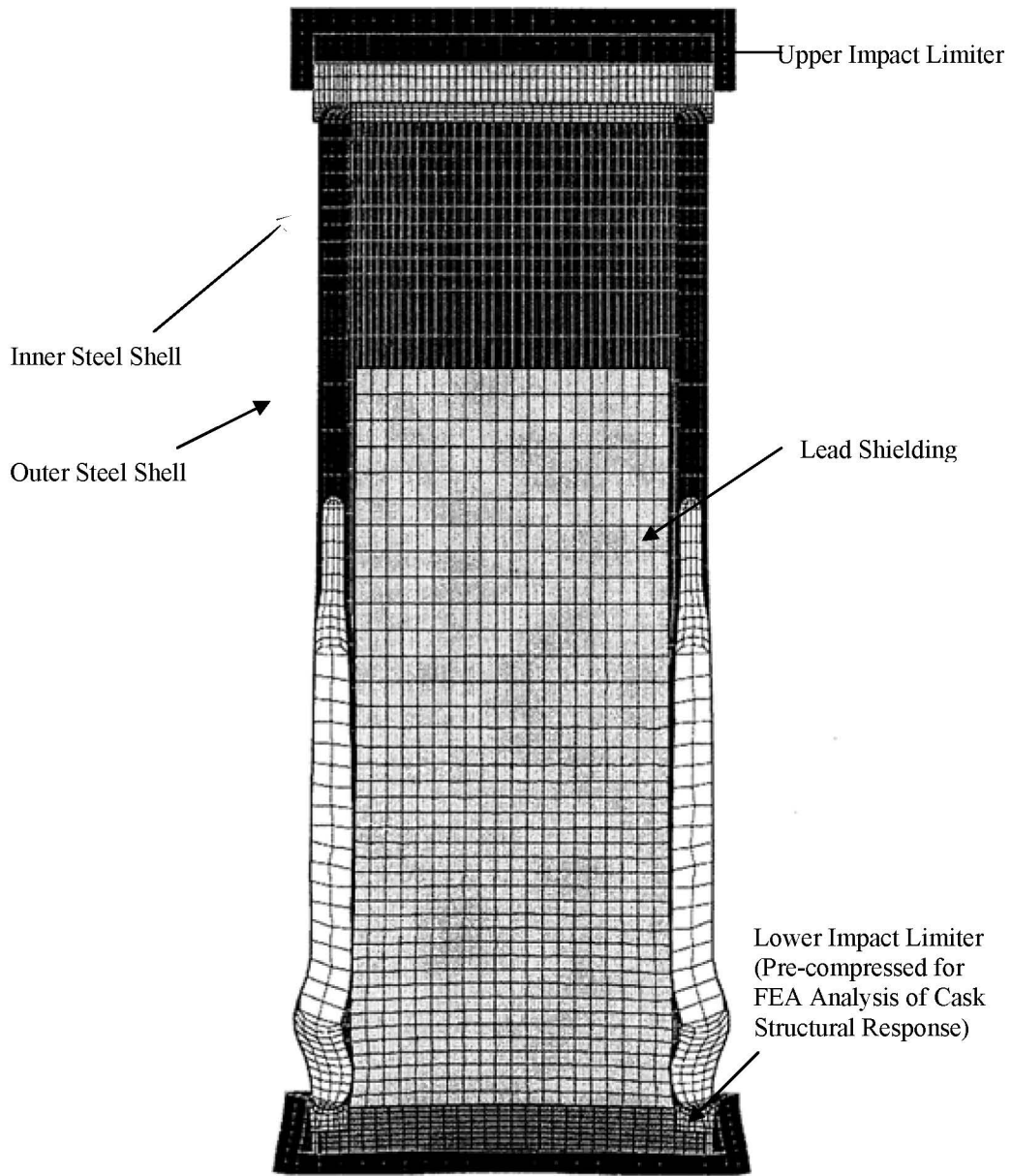
Two horizontal lines were superimposed on Figures D3.2-2 and D3.2-3 to plot the 0.2% and 2.0% strain to represent the respective S2 and S3 thresholds for inner shell strain. The intersections of the strain curves with the respective threshold values indicate the minimum impact speed at which the respective S2 and S3 strain thresholds appear to be exceeded.

Table D3.2-1. Maximum Plastic Strain in Inner Shell of Sandwich Wall Casks

Cask Type	Orientation: Speed, mph	Corner Impact Strain, %	End Impact Strain, %	Side Impact Strain, %
SLS Truck	30	12	3.9	N/A
	60	29	12	16
	90	33	18	24
	120	47	27	27
SDUS Truck	30	11	1.8	6
	60	27	4.8	13
	90	43	8.3	21
	120	55	13	30
SLS Rail	30	21	1.9	5.9
	60	34	5.5	11
	90	58	13	15
	120	70	28	N/A

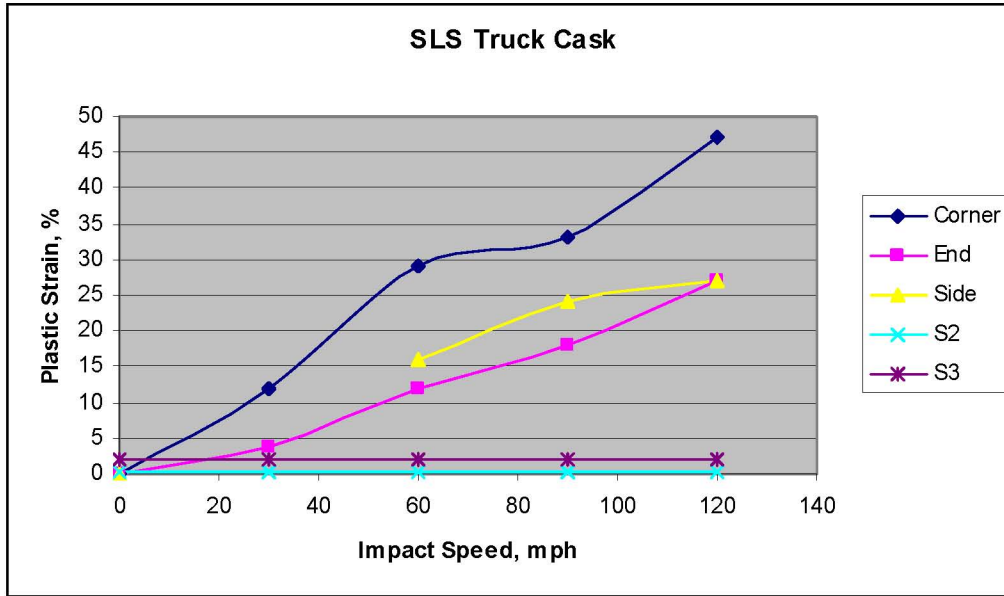
NOTE: SDU = steel-depleted uranium-steel; SLS = steel-lead-steel.

Source: From Ref. D4.1.65, Table 5.3



Source: From Ref. D4.1.65, Figure 5.9

Figure D3.2-1. Illustration of Deformation and Lead Slumping for a SLS Rail Cask Following End-on Impact at 120 mph

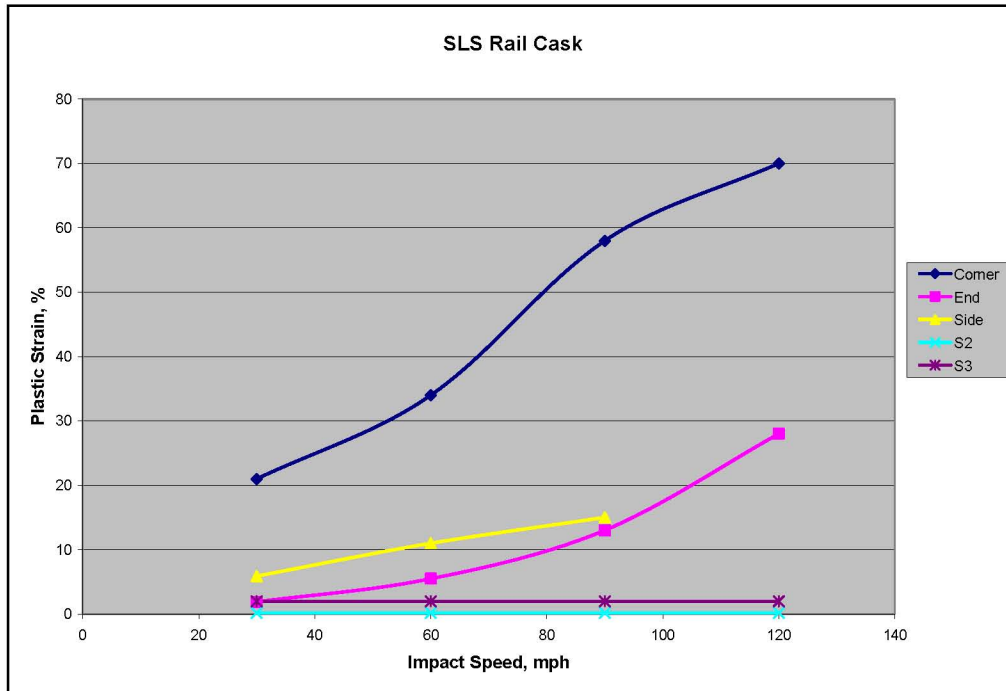


NOTE: ¹ Data points for strain versus speeds greater than 30 mph taken directly from NUREG/CR-6672, Table 5.3: plots extended to origin (0,0) to determine crossover for S2 and S3 threshold strains.
² S2 and S3 threshold strains based on information in *A Railroad Industry Critique of the Model Study* (Ref. D4.1.30).

mph = miles per hour; SLS = steel-lead-steel.

Source: Original

Figure D3.2-2. Truck Steel/Lead/Steel Inner Shell Strain versus Impact Speed



NOTE: ¹ Data points for strain versus speeds greater than 30 mph taken directly from NUREG/CR-6672 (Ref. D4.1.65, Table 5.3): plots extended to origin (0,0) to determine crossover for S2 and S3 threshold strains.

² S2 and S3 threshold strains based on information in *A Railroad Industry Critique of the Model Study* (Ref. D4.1.30).

mph = miles per hour; SLS = steel-lead-steel.

Source: Original

Figure D3.2-3. Rail Steel/Lead/Steel Strain versus Impact Speed

D3.3 ESTIMATE OF THRESHOLD SPEEDS FOR LOSS OF SHIELDING DUE TO IMPACTS

The plots in Figures D3.2-2 and D3.2-3, and Table D3.2-1 illustrate that the S2 threshold is exceeded for both the truck and rail SLS casks for all four speed ranges and all orientations. Since NUREG/CR-6672 (Ref. D4.1.65) does not report LOS conditions for low impact speeds, it is concluded that the S2 criterion is not a valid threshold for LOS in SLS casks. Therefore, the remainder of this analysis applies the S3 criterion (2% shell strain) as a basis for estimating LOS threshold impact speeds.

Figures D3.2-2 and D3.2-3, and Table D3.2-1 indicate that the S3 threshold is exceeded for both truck and rail SLS casks for all orientations. The intersections of the strain curves and the 2% strain line in Figures D3.2-2 and D3.2-3 illustrate the impact speed at where the S3 threshold is reached for each case. A small exception being the end drop of a SLS rail cask in the 30-60 mph range for which the shell strain of 1.9% is just below the lower bound for S3 damage. However, this margin is too small to exclude that case. Although the strains for the side drop cases exceed the threshold for lead slumping, NUREG/CR-6672 (Ref. D4.1.65) states that lead

slumping does not occur in side drops. Therefore, LOS for side drops is excluded from the remainder of this report.

Using the 2% shell strain condition as the threshold for LOS in SLS casks, the following is observed:

- LOS for the truck SLS cask would occur at impact speeds of about 5 mph for corner impact and about 18 mph for end impact
- LOS for the rail SLS cask would occur at about 3 mph for corner impact and about 30 mph for end impact.

It is observed that the corner drop cases give the largest shell strain at a given impact speed but the finite element analyses indicate that the extent of lead slumping is less in corner drops than for end impacts.

Table D3.3-1 shows the drop height equivalents for impact speed onto a horizontal unyielding surface. Thus, to exceed 5 mph, for example, a drop height greater than 0.8 ft is required; to exceed 30 mph impact, a drop height greater than 30 ft is required. Using the results cited above:

- LOS for the truck SLS cask would occur at impact speeds of about 0.8 ft (5 mph) for corner impact and about 10 ft (18 mph) for end impact
- LOS for the rail SLS cask would occur at about 0.5 ft (3 mph) for corner impact and about 30 ft (30 mph) for end impact.

Such drop heights could occur in some GROA handling operations.

However, when the effect of the energy absorption by real targets is considered, much greater impact speeds are required to impose the damage equivalent to impacts on unyielding targets. NUREG/CR-6672 (Ref. D4.1.65) provides a correlation of impact speeds for real versus unyielding target, but provides only bounding values for a large number of cases as presented in Table D3.3-2. Therefore, if LOS occurs at 30 mph for an end drop of a SLS train cask on unyielding surface, a speed of greater than 150 mph is required for an impact on concrete. This impact speed would require a drop of over 500 ft. Such drop heights cannot be achieved in repository handling.

Some of the LOS cases, including corner drops of truck and rail SLS casks, appear to result in LOS for impact speeds less than 10 mph. If the corner drops are onto concrete, a speed of 2 to 3 times the threshold speed for LOS for impact on an unyielding target. This implies a threshold impact speed of 20 to 30 mph for a corner drop onto concrete. The corresponding drop height is 13 feet to 30 feet. Such drops could occur in event sequences for repository handling.

Table D3.3-1. Drop Height to Reach a Given Impact Speed

Impact Speed, mph	Equivalent Drop Height, ft
2	0.1
5	0.8
10	3.3
20	13.4
30	30.1
40	53.4
50	83.5
60	120.2
70	163.7
80	213.8
90	270.6
100	334.0
110	404.2
120	481.0

Source: Original

Table D3.3-2. Impact Speeds on Real Target for Equivalent Damage for Unyielding Targets

Cask Type	Real Target type	Impact Type\Orientation w/o Impact Limiters	Impact Speed , mph			
			30	60	90	120
Rail SLS	Soil	End	>>150	>>150	>>150	>>150
		Side	72	>150	>>150	>>150
		Corner	68	133	>150	>150
	Concrete slab	End	>150	>>150	>>150	>>150
		Side	85	>150	>>150	>>150
		Corner	>>150	>>150	>>150	>>150
Truck SLS	Soil	End	>150	>>150	>>150	>>150
		Side	70	>150	>>150	>>150
		Corner	61	>150	>>150	>>150
	Concrete slab	End	123	180	>>150	>>150
		Side	35	86	135	>150
		Corner	56	123	>150	>>150

NOTE: mph = miles per hour; SLS = steel-lead-steel.

Source: Based on NUREG/CR-6672 (Ref. D4.1.65, Tables 5.10 and 5.12)

D3.4 PROBABILITY OF LOSS OF SHIELDING

NUREG/CR-6672 (Ref. D4.1.65) develops probabilities for LOS in transportation accidents. The probability of LOS uses event tree analysis with split fractions for various types of transportation accidents and frequencies based on accident rates per mile of travel for cask-bearing truck trailers or rail cars. The results of probability analyses of LOS as derived in

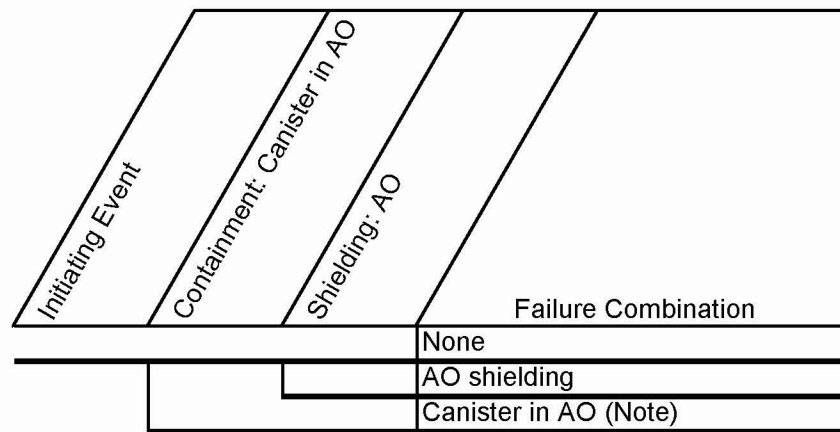
NUREG/CR-6672 (Ref. D4.1.65) do not have any direct relevance to event sequences for waste handling operations. However, the basic approach that breaks down the overall probability of an event sequence involving LOS into conditional probabilities for occurrence of various physical conditions that lead to LOS can be adapted for PCSA.

The vulnerability to LOS for repository event sequences varies with the container type:

1. Concrete overpack with no containment boundary (aging overpack)
2. Sandwich type with steel containment boundary and lead in the annulus between the steel shells (transportation cask).
3. All other casks including monolithic steel casks or casks with layers of steel or steel and depleted uranium (transportation cask, shielded transfer cask (STC)).

Concrete Overpacks

Aging overpacks provide shielding but not containment. They are used within the GROA to transport DPCs and TAD canisters between buildings and to and from the aging pads. The event sequences that involve both are of the form shown in Figure D3.4-1 below.



Note: Implies shielding is ineffective because of radionuclide release

NOTE: AO = aging overpack

Source: Original

Figure D3.4-1. Summary Event Tree Showing Model Logic for Canisters and Aging Overpacks

A site transporter transports aging overpacks with canisters within the GROA. The transporter is designed for a maximum speed of 2.5 mph (Ref. D4.1.18, Sections 3.2.1 and 3.2.4) and will elevate the aging overpack no more than 3 feet from the ground (equipment limit is 12 inches (Ref. D4.1.18, Section 2.2, item 9)), additional two feet is allowed for potential drop off edge of aging pad). Expanding the probability of success (no breach) of a canister within an aging overpack yields:

$$p_{AO}(C) = p_{AO}(C | O)p_{AO}(O) + p_{AO}(C | \bar{O})p_{AO}(\bar{O}), \quad (\text{Eq. D-26})$$

where

$p_{AO}(C)$ = probability of canister success within an AO.

$p_{AO}(C | O)$ = probability of canister success given AO shielding does not fail.

$p_{AO}(O)$ = probability that AO shielding does not fail.

$p_{AO}(C | \bar{O})$ = probability of canister success given AO shielding fails.

$p_{AO}(\bar{O})$ = probability that AO shielding fails.

The inner and outer steel lined 3 foot concrete aging overpack is much more robust against impact loads than a DPC. Therefore, if the overpack fails, it is much more likely that the canister will breach. This yields: $p_{AO}(C | O) \gg p_{AO}(C | \bar{O})$. Furthermore, the probability of aging overpack breach is much less than probability of aging overpack success at the above drop and speed conditions. Therefore: $p_{AO}(O) \gg p_{AO}(\bar{O})$. The second term on the right hand side of Equation D-26 is much less than the first term and need not be considered further in this analysis.

This leaves

$$p_{AO}(C) \cong p_{AO}(C | O)p_{AO}(O) \quad (\text{Eq. D-27})$$

Note that

$$\begin{aligned} p_{AO}(C) = 1 - p_{AO}(\bar{C}) \quad \text{and} \quad p_{AO}(O) = 1 - p_{AO}(\bar{O}) \quad \text{and} \\ p_{AO}(C | O) = 1 - p_{AO}(\bar{C} | O) \end{aligned} \quad (\text{Eq. D-28})$$

Substituting Equations D-28 into D-27 and rearranging yields:

$$p_{AO}(\bar{O}) \cong 1 - \frac{1 - p_{AO}(\bar{C})}{1 - p_{AO}(\bar{C} | O)} \quad (\text{Eq. D-29})$$

LLNL has developed a mean probability of failure for a canister within an aging overpack, $p_{AO}(\bar{C})$, for a 3-foot drop onto a rigid surface with an initial velocity of 2.5 mph (Ref. D4.1.27).

This analysis uses a conservative value of 1E-05 relative to the 1E-08 value in the referenced LLNL report. The probability of canister failure given the aging overpack does not fail, $p_{AO}(\bar{C} | O)$, must be less than the overall probability of canister failure within an aging overpack, $p_{AO}(\bar{C})$. It is, therefore, reasonable to use a range of values of 1E-06 to 1E-05 for this, both of which are conservative relative to the value in the reference. The LLNL (Ref. D4.1.27) value, itself, has a conservative element in that it analyzes impact onto a rigid surface. The more realistic concrete surface would have a lower canister failure probability. Using the average between 1E-06 and 1E-05 of 5E-06 for $p_{AO}(\bar{C} | O)$ and also substituting the aforementioned value for $p_{AO}(\bar{C})$ into Equation D-29, there obtains:

$$p_{AO}(\bar{O}) \cong 1 - \frac{1 - p_{AO}(\bar{C})}{1 - p_{AO}(\bar{C} | O)} = 1 - \frac{1 - 10^{-5}}{1 - 5 \times 10^{-6}} = 5 \times 10^{-6} \quad (\text{Eq. D-30})$$

Steel/Lead/Steel Sandwich-Type Casks

For these sandwich-type casks, the probability of LOS due to lead slumping can be estimated from results of transportation cask studies that can be coupled to event sequence probability analysis and insights from the passive failure analyses. Since the speed of transport of transportation casks to, and within, the processing facilities is limited to a few mph, it is judged that LOS of SLS casks (and the other types) may be screened out from collision scenarios. However, LOS for SLS casks due to drops cannot be ruled out, if SLS casks are processed in the repository.

For SLS casks, the probability of LOS is derived from the probability that the drop height or impact speed exceeds the threshold at which lead shielding may slump. For all cask types, the probability of LOS is derived from the probability that the drop height or impact speed exceeds the threshold at which cask closure and/or seals fail in such a way to permit to permit direct streaming. A simplified conservative approach to estimating the probability of LOS due to lead slumping resulting from a drop of an SLS cask is summarized in the next section.

The PCSA considers drop and collision event sequences of transportation casks. Should a canister rupture occur, the analysis conservatively models the shielding as also lost. In such event sequences the probability of loss of shielding is taken to be 1.0 given canister rupture. This applies to all types of casks.

Event sequences also include LOS without canister rupture. That is, the drop or collision was not severe enough to cause a rupture but a LOS is possible in some casks. Such an event sequence can not occur in the steel/depleted uranium truck casks. The loss of shielding associated with streaming through the head of steel monolith rail casks is due to structural failure of the casks. The probability of this is estimated by taking the breach/rupture probability of a steel monolith transportation cask at the weakest location and applying it as a head rupture probability.

Collisions of casks will occur at less than 5 mph. Drops can occur as high as 30 feet. Drops may be at any orientation: side, bottom, and end. A conservative approach to estimation of the probability of SLS LOS is to use the information associated with end drops, which can cause bulging of the steel containment that allows the lead to collect towards one end. Although the corner impact can cause greater strain in the steel containment, it does not cause the spreading that increases collection of the lead at one end. All surfaces in the repository upon which a transportation cask can be dropped (concrete or soil) are concrete or softer. Therefore, the concrete related drop height vs. LOS information may be accurately used.

An impact of at least 123 mph against a real surface such as concrete or soil is required in order to cause the same damage as an impact of 30 mph against an unyielding surface (Table D3.3-2). The vast majority of casks are to be delivered to the repository by rail. The maximum strain due to an end impact of 30 mph against an unyielding surface, or 123 mph against a real surface, is about 3.9% for a truck cask (greater than the 1.9% strain for a rail cask) (Table D3.2-1). Noting in Figure D3.2-3 that the amount of strain is roughly linear with the impact velocity, a velocity of 63 mph is estimated to correspond to the strain of 2% indicative of S3 damage and lead slumping. A 63 mph collision, equivalent to a 133-foot drop, is the threshold for causing enough damage to indicate potential loss of shielding due to lead slumping.

In order to develop fragility over height, the available information described herein indicates that an estimate of a median threshold for a failure drop height is 133 feet. This would yield 2% strain. A coefficient variation (the ratio of standard deviation to the median) is 0.1. This is an estimate derived from the distribution of capacity associated with the tensile strength elongation data described in Section D1.1. The probability of LOS due to lead slumping resulting from a 15-foot vertical drop would be less than 1×10^{-8} , given the drop event. For a 30-foot drop resulting from a 2-blocking event, the computed failure probability based on the 133-foot median drop height is also less than 1×10^{-8} . LOS due to lead slumping applies only to those casks using lead for shielding but the PCSA applied this analysis to all casks. A conservative value of 1×10^{-5} is used to be consistent with the probabilities based on the LLNL (Ref. D4.1.27) results.

Results are shown in Tables D3.4-1.

Table D3.4-1. Probabilities of Degradation or Loss of Shielding

	Probability	Note
Sealed transportation cask and shielded transfer casks shielding degradation after structural challenge	1×10^{-5}	Section D3.4
Aging overpack shielding loss after structural challenge	5×10^{-6}	Section D3.4
CTM shielding loss after structural challenge	0	Structural challenge sufficiently mild to leave the shielding function intact ^a
WPTT shielding loss after structural challenge	0	Structural challenge sufficiently mild to leave the shielding function intact ^a
TEV shielding loss (shield end)	0	Structural challenge sufficiently mild to leave the shielding function intact ^a
Shielding loss by fire for waste forms in transportation casks or shielded transfer casks	1	Lead shielding could potentially expand and degrade. This probability is conservatively applied to transportation casks and STCs that do not use lead for shielding
Shielding loss by fire of aging overpacks, CTM shield bell, and WPTT shielding	0	Type of concrete used for aging overpacks is not sensitive to spallation; Uranium used in CTM shield bell and WPTT shielding does not lose its shielding function as a result of fire

NOTE: ^a In the event sequence diagrams of the PCSA, the shielding function for the CTM, WPTT and TEV is queried for the challenges that do not lead to a radioactive release. Such challenges, which were not sufficiently severe to cause a breach of containment of the waste form container, are also deemed mild enough to leave the shielding function of the CTM, WPTT and TEV intact.

CTM = canister transfer machine; STC = shielded transfer cask; TEV=transport and emplacement vehicle; WPTT = waste package transfer trolley.

Source: Original

All Other Cask Types

For all other cask types, the results of the transportation cask study indicate that the only mechanism for LOS is streaming via closure failures and closure geometry changes. Therefore, the probability of LOS can be equated to the probability of rupture/breach of such casks.

D4 REFERENCES

D4.1 DESIGN INPUTS

The PCSA is based on a snapshot of the design. The reference design documents are appropriately documented as design inputs in this section. Since the safety analysis is based on a snapshot of the design, referencing subsequent revisions to the design documents (as described in EG-PRO-3DP-G04B-00037, *Calculations and Analyses* (Ref. 2.1.1, Sections 3.2.1 and 3.2.2.F)) that implement PCSA requirements flowing from the safety analysis would not be appropriate for the purpose of this document. There are no superseded or cancelled documents associated with the modifications that led to the issuance of this revision. Cancelled or superseded documents associated with the portions of this document for which the snapshot has not yet been updated are designated herein with a dagger (†).

The inputs in this section noted with an asterisk (*) indicate that they fall into one of the designated categories described in Section 4.1, relative to suitability for intended use.

- D4.1.1* Allegheny Ludlum 2006. “Technical Data Blue Sheet, Stainless Steels Chromium-Nickel-Molybdenum, Types 316 (S31600), 316L (S31603), 317 (S31700), 317L (S31703).” Technical Data Blue Sheet. Brackenridge, Pennsylvania: Allegheny Ludlum. TIC: 259471. LC Call Number: TA 486. A4 2006.
- D4.1.2* A.M. Birk Engineering 2005. *Tank Car Thermal Protection Defect Assessment: Updated Thermal Modelling with Results of Fire Testing*. TP 14367E. Ontario, Canada: Transportation Development Centre of Transport Canada. ACC: MOL.20071113.0095.
- D4.1.3* ASM (American Society for Metals) 1961. “Properties and Selection of Metals.” Volume 1 of *Metals Handbook*. 8th Edition. Lyman, T.; ed. Metals Park, Ohio: American Society for Metals. TIC: 257281. LC Call Number: TA459 .M43 1961 Vol.1.
- D4.1.4* ASM 1976. *Source Book on Stainless Steels*. Metals Park, Ohio: American Society for Metals. TIC: 259927. LC Call Number: TA479 .S7 S64 1976.
- D4.1.5* ASME (American Society of Mechanical Engineers) 2001. *2001 ASME Boiler and Pressure Vessel Code (includes 2002 addenda)*. New York, New York: American Society of Mechanical Engineers. TIC: 251425.
- D4.1.6* ASME 2004. *2004 ASME Boiler and Pressure Vessel Code*. 2004 Edition. New York, New York: American Society of Mechanical Engineers. TIC: 256479.
- D4.1.7* ASTM (American Society for Testing and Materials) G 1-03. 2003. *Standard Practice for Preparing, Cleaning, and Evaluating Corrosion Test Specimens*. West Conshohocken, Pennsylvania: American Society for Testing and Materials. TIC: 259413.

- D4.1.8* Avallone, E.A. and Baumeister, T., III, eds. 1987. *Marks' Standard Handbook for Mechanical Engineers*. 9th Edition. New York, New York: McGraw-Hill. TIC: 206891. ISBN: 0-07-004127-X.
- D4.1.9* BNFL Fuel Solutions 2003. *FuelSolutions™ TS125 Transportation Cask Safety Analysis Report, Revision 5*. Document No. WSNF-120. Docket No. 71-9276. Campbell, California: BNFL Fuel Solutions. TIC: 257634.
- D4.1.10 Not used.
- D4.1.11† BSC 2006. *CRCF, IHF, RF, and WHF Canister Transfer Machine Mechanical Equipment Envelope*. 000-MJ0-HTC0-00201-000 REV 00A. Las Vegas, Nevada: Bechtel SAIC Company. ACC: ENG.20061120.0011.
- D4.1.12† BSC 2007. *Mechanical Handling Design Report: Waste Package Transport and Emplacement Vehicle*. 000-30R-HE00-00200-000 REV 001. Las Vegas, Nevada: Bechtel SAIC Company. ACC: ENG.20071205.0002.
- D4.1.13 BSC 2007. *5-DHLW/DOE SNF - Long Co-Disposal Waste Package Configuration*. 000-MW0-DS00-00203-000 REV 00C. Las Vegas, Nevada: Bechtel SAIC Company. ACC: ENG.20070719.0007.
- D4.1.14 BSC 2007. *Aging Facility Vertical DPC Aging Overpack Mechanical Equipment Envelope Sheet 1 of 2*. 170-MJ0-HAC0-00201-000 REV 00B. Las Vegas, Nevada: Bechtel SAIC Company. ACC: ENG.20070928.0032.
- D4.1.15† BSC 2007. *Basis of Design for the TAD Canister-Based Repository Design Concept*. 000-3DR-MGR0-00300-000-001. Las Vegas, Nevada: Bechtel SAIC Company. ACC: ENG.20071002.0042.
- D4.1.16* BSC 2007. *Discipline Design Guide and Standards for Surface Facilities HVAC Systems*. 000-3DG-GEHV-00100-000-00A. Las Vegas, Nevada: Bechtel SAIC Company. ACC: ENG.20070514.0007.
- D4.1.17 BSC 2007. *Leak Path Factors for Radionuclide Releases from Breached Confinement Barriers and Confinement Areas*. 000-00C-MGR0-01500-000-00A. Las Vegas, Nevada: Bechtel SAIC Company. ACC: ENG.20071018.0002.
- D4.1.18† BSC 2007. *Mechanical Handling Design Report - Site Transporter*. 170-30R-HAT0-00100-000-000. Las Vegas, Nevada: Bechtel SAIC Company. ACC: ENG.20071217.0015.
- D4.1.19 BSC 2007. *Naval Long Oblique Impact Inside TEV*. 000-00C-DNF0-01200-000-00A. Las Vegas, Nevada: Bechtel SAIC Company. ACC: ENG.20070806.0016.
- D4.1.20 BSC 2007. *Naval Long Waste Package Vertical Impact on Emplacement Pallet and Invert*. 000-00C-DNF0-00100-000-00C. Las Vegas, Nevada: Bechtel SAIC Company. ACC: ENG.20071017.0001.

- D4.1.21 BSC 2007. *Probabilistic Characterization of Preclosure Rockfalls in Emplacement Drifts*. 800-00C-MGR0-00300-000-00A. Las Vegas, Nevada: Bechtel SAIC Company. ACC: ENG.20070329.0009.
- D4.1.22 BSC 2007. *TAD Waste Package Configuration*. 000-MW0-DSC0-00101-000 REV 00B. Las Vegas, Nevada: Bechtel SAIC Company. ACC: ENG.20070301.0010.
- D4.1.23 BSC 2007. *TAD Waste Package Configuration*. 000-MW0-DSC0-00102-000 REV 00B. Las Vegas, Nevada: Bechtel SAIC Company. ACC: ENG.20070301.0011.
- D4.1.24 BSC 2007. *TAD Waste Package Configuration*. 000-MW0-DSC0-00103-000 REV 00B. Las Vegas, Nevada: Bechtel SAIC Company. ACC: ENG.20070301.0012.
- D4.1.25 BSC 2007. *Thermal Responses of TAD and 5-DHLW/DOE SNF Waste Packages to a Hypothetical Fire Accident*. 000-00C-WIS0-02900-000-00A. Las Vegas, Nevada: Bechtel SAIC Company. ACC: ENG.20070220.0008.
- D4.1.26 BSC 2007. *Waste Package Capability Analysis for Nonlithophysal Rock Impacts*. 000-00C-MGR0-04500-000-00A. Las Vegas, Nevada: Bechtel SAIC Company. ACC: ENG.20071113.0017.
- D4.1.27 BSC 2008. *Seismic and Structural Container Analyses for the PCSA*. 000-PSA-MGR0-02100-000-00A. Las Vegas, Nevada: Bechtel SAIC Company. ACC: ENG.20080220.0003.
- D4.1.28 DOE (U.S. Department of Energy) 2007. *Transportation, Aging and Disposal Canister System Performance Specification*. WMO-TADCS-000001, Rev. 0. Washington, D.C.: U.S. Department of Energy, Office of Civilian Radioactive Waste Management. ACC: DOC.20070614.0007. (DIRS 181403)
- D4.1.29 DOE 2008. *Quality Assurance Requirements and Description*. DOE/RW-0333P, Rev. 20. Washington, D. C.: U.S. Department of Energy, Office of Civilian Radioactive Waste Management. ACC: DOC.20080205.0001.
- D4.1.30* English, G.W.; Moynihan, T.W.; Worswick, M.J.; Birk, A.M. 1999. *A Railroad Industry Critique of the Model Study*. 96-025-TSD. Kingston, Ontario, Canada: Association of American Railroads Safety & Operations. TIC: 260032. LC Call Number: TK9152.17 .T73 1999.
- D4.1.31* Evans, D.D. 1993. "Sprinkler Fire Suppression Algorithm for HAZARD." *Fire Research and Safety, 12th Joint Panel Meeting, October 27-November 2, 1992, Tsukuba, Japan*. Pages 114-120. Tsukuba, Japan: Building Research Institute and Fire Research Institute. ACC: MOL.20071114.0163.

- D4.1.32* Fischer, L.E.; Chou, C.K.; Gerhard, M.A.; Kimura, C.Y.; Martin, R.W.; Mensing, R.W.; Mount, M.E.; and Witte, M.C. 1987. *Shipping Container Response to Severe Highway and Railway Accident Conditions*. NUREG/CR-4829. Two volumes. Washington, D.C.: U.S. Nuclear Regulatory Commission. ACC: NNA.19900827.0230; NNA.19900827.0231.
- D4.1.33* Friedrich, T. and Schellhaas, H. 1998. *Computation of the percentage points and the power for the two-sided Kolmogorov-Smirnov one sample test*. Statistical Papers 39:361-75. TIC: 260013.
- D4.1.34* General Atomics. 1995. *GA-9 Legal Weight Truck From-Reactor Spent Fuel Shipping Cask, Final Design Report (FDR)*. 910354 N/C. San Diego, California: General Atomic. ACC: MOV.20000106.0003.
- D4.1.35* Haynes International 1990. *Reliability and Longevity of Furnace Components as Influenced by Alloy of Construction*. H-3124. Kokomo, Indiana: Haynes International. TIC: 256362.
- D4.1.36* Haynes International 1997. *Hastelloy C-22 Alloy*. Kokomo, Indiana: Haynes International. TIC: 238121.
- D4.1.37* Hertz, K.D. 2003. "Limits of Spalling of Fire-Exposed Concrete." *Fire Safety Journal*, 38, 103-116. [New York, New York]: Elsevier. TIC: 259993.
- D4.1.38* Holtec International 2003. *Storage, Transport, and Repository Cask Systems, (Hi-Star Cask System) Safety Analysis Report, 10 CFR 71, Docket 71-9261*. HI-951251, Rev. 10. Marlton, New Jersey: Holtec International. ACC: MOL.20050119.0271.
- D4.1.39* Holtec International 2005. *Final Safety Analysis Report for the HI-STORM 100 Cask System*. USNRC Docket No.: 72-1014. Holtec Report No.: HI-2002444. Marlton, New Jersey: Holtec International. TIC: 258829.
- D4.1.40* Hubbell, J.H. and Seltzer, S.M., *Tables of X-Ray Mass Attenuation Coefficients and Mass Energy-Absorption Coefficients* (version 1.4). National Institute of Standards and Technology, Gaithersburg, MD, 2004. (Originally published as NISTIR 5632, National Institute of Standards and Technology, Gaithersburg, MD, 1995) (Available online at: <http://physics.nist.gov/PhysRefData/XrayMassCoef/tab4.html>) ACC: MOL.20080303.0046.
- D4.1.41* Incropera, F.P. and DeWitt, D.P. 1996. *Introduction to Heat Transfer*. 3rd Edition. New York, New York: John Wiley and Sons. TIC: 241057. ISBN: 0-471-30458-1.
- D4.1.42 Not used.
- D4.1.43* Kodur, V.K.R.; Wang, T.C.; and Cheng, F.P. 2004. "Predicting the Fire Resistance Behaviour of High Strength Concrete Columns." *Cement & Concrete Composites*, 26, 141-153. [New York, New York]: Elsevier. TIC: 259996.

- D4.1.44* Larson, F.R. and Miller, J. 1952. "A Time-Temperature Relationship for Rupture and Creep Stresses." *Transactions of the American Society of Mechanical Engineers*, 74, 765-775. New York, New York: American Society of Mechanical Engineers. TIC: 259911.
- D4.1.45 Lide, D.R., ed. 1995. *CRC Handbook of Chemistry and Physics*. 76th Edition. Boca Raton, Florida: CRC Press. TIC: 216194. ISBN: 0-84930476-8.
- D4.1.46* Majumdar, S.; Shack, W.J.; Diercks, D.R.; Mruk, K.; Franklin, J.; and Knoblich, L. 1998. *Failure Behavior of Internally Pressurized Flawed and Unflawed Steam Generator Tubing at High Temperatures – Experiments and Comparisons with Model Predictions*. NUREG/CR-6575. Washington, D.C.: Nuclear Regulatory Commission. ACC: MOL.20071106.0053.
- D4.1.47* Mason, M. 2001. "NUHOMS-MP197 Transport Packaging Safety Analysis Report." Letter from M. Mason (Transnuclear) to E.W. Brach (NRC), May 2, 2001, E-21135, with enclosures. TIC: 255258.
- D4.1.48* Morris Material Handling 2008. *Mechanical Handling Design Report - Canister Transfer Machine*. V0-CY05-QHC4-00459-00018-001-004. Oak Creek, Wisconsin: Morris Material Handling. ACC: ENG.20080121.0010.
- D4.1.49* NAC (Nuclear Assurance Corporation) 2000. *Safety Analysis Report for the NAC Legal Weight Truck Cask*. Revision 29. Docket No. 71-9225. T-88004. Norcross, Georgia: Nuclear Assurance Corporation International. ACC: MOL.20070927.0003.
- D4.1.50* NAC (Nuclear Assurance Corporation) 2004. "NAC-STC NAC Storage Transport Cask, Revision 15." Volume 1 of *Safety Analysis Report*. Docket No. 71-9235. Norcross, Georgia: NAC International. TIC: 257644.
- D4.1.51* Nakos, J.T. 2005. *Uncertainty Analysis of Steady State Incident Heat Flux Measurements in Hydrocarbon Fuel Fires*. SAND2005-7144. Albuquerque, New Mexico: Sandia National Laboratories. ACC: MOL.20071106.0054.
- D4.1.52* Nowlen, S.P. 1986. *Heat and Mass Release for Some Transient Fuel Source Fires: A Test Report*. NUREG/CR-4680. SAND86-0312. Washington, D.C.: U.S. Nuclear Regulatory Commission. ACC: MOL.20071113.0099.
- D4.1.53* Nowlen, S.P. 1987. *Quantitative Data on the Fire Behavior of Combustible Materials Found in Nuclear Power Plants: A Literature Review*. NUREG/CR-4679. SAND86-0311. Washington, D.C.: U.S. Nuclear Regulatory Commission. ACC: MOL.20071113.0100.
- D4.1.54* NRC (U.S. Nuclear Regulatory Commission) 1997. *Standard Review Plan for Dry Cask Storage Systems*. NUREG-1536. Washington, D.C.: U.S. Nuclear Regulatory Commission. ACC: MOL.20010724.0307.

- D4.1.55* NRC 2003. *Interim Staff Guidance - 18. The Design/Qualification of Final Closure Welds on Austenitic Stainless Steel Canisters as Confinement Boundary for Spent Fuel Storage and Containment Boundary for Spent Fuel Transportation.* ISG-18. Washington, D.C.: U.S. Nuclear Regulatory Commission. TIC: 254660.
- D4.1.56* NRC 2007. *Interim Staff Guidance HLWRS-ISG-02, Preclosure Safety Analysis - Level of Information and Reliability Estimation.* HLWRS-ISG-02. Washington, D.C.: U.S. Nuclear Regulatory Commission. ACC: MOL.20071018.0240.
- D4.1.57* Quintiere, J.G. 1998. *Principles of Fire Behavior.* Albany, New York: Delmar Publishers. TIC: 251255. ISBN: 0-8273-7732-0.
- D4.1.58* Rieth, M.; Falkenstein, A.; Graf, P.; Heger, S.; Jäntschi, U.; Klimiankou, M.; Materna-Morris, E.; and Zimmermann, H. 2004. *Creep of the Austenitic Steel AISI 316L(N), Experiments and Models.* FZKA 7065. Karlsruhe, Germany: Forschungszentrum Karlsruhe GmbH. TIC: 259943.
- D4.1.59* Sasikala, G.; Mathew, M.D.; Bhanu Sankara Rao, K.; and Mannan, S.L. 1997. "Assessment of Creep Behaviour of Austenitic Stainless Steel Welds." *Creep-Fatigue Damage Rules for Advanced Fast Reactor Design, Proceedings of a Technical Committee Meeting, Manchester, United Kingdom, 11-13 June 1996.* IAEA-TECDOC-993. Pages 219-227. Vienna, Austria: International Atomic Energy Agency. TIC: 259880.
- D4.1.60* Savolainen, K.; Mononen, J.; Ilola, R.; Hanninen, H. 2005. *Materials Selection for High Temperature Applications [TKK-MTR-4/05].* TKK-MTR-4/05. Helsinki, Finland, Espoo, Finland: Helsinki University of Technology, Laboratory of Engineering Materials; Otamedia Oy. TIC: 259896. ISBN: 951-22-7892-8.
- D4.1.61* Society of Fire Protection Engineering (SFPE) 1988. *The SFPE Handbook of Fire Protection Engineering, Society of Fire Protection Engineers.* Edition 1. Boston, MA: Society of Fire Protection Engineering (SFPE). TIC: 101351. ISBN: 0-87765-353-4.
- D4.1.62* Shapiro, S. S. and Wilk, M. B. 1965. "An Analysis of Variance Test for Normality (Complete Samples)." *Biometrika*, 52 (3 - 4), 591-611. Cary, North Carolina: Oxford University Press. TIC: 259992.
- D4.1.63* Siegel, R. and Howell, J.R. 1992. *Thermal Radiation Heat Transfer.* 3rd Edition. Washington, D.C.: Taylor & Francis. TIC: 236759. ISBN: 0-89116-271-2. (Radiation view factors also available online at: <http://www.me.utexas.edu/~howell/index.html>.)
- D4.1.64* Snow, S.D. 2007, *Structural Analysis Results of the DOE SNF Canisters Subjected to the 23-Foot Vertical Repository Drop Event to Support Probabilistic Risk Evaluations,* EDF-NSNF-085, Rev. 0. Idaho Falls, Idaho: Idaho National Laboratory. ACC: MOL.20080206.0062.

D4.1.65* Sprung, J.L.; Ammerman, D.J.; Breivik, N.L.; Dukart, R.J.; Kanipe, F.L.; Koski, J.A.; Mills, G.S.; Neuhauser, K.S.; Radloff, H.D.; Weiner, R.F.; and Yoshimura, H.R. 2000. *Reexamination of Spent Fuel Shipment Risk Estimates*. NUREG/CR-6672. Two volumes. Washington, D.C.: U.S. Nuclear Regulatory Commission. ACC: MOL.20001010.0217.

D4.1.66* Transnuclear 2001. *TN-68 Transport Packaging Safety Analysis Report, Revision 4*. Hawthorne, New York: Transnuclear. TIC: 254025.

D4.2 DESIGN CONSTRAINTS

D4.2.1 10 CFR 20. 2007. Energy: Standards for Protection Against Radiation.

D4.2.2 10 CFR 71. 2007. Energy: Packaging and Transportation of Radioactive Material.

INTENTIONALLY LEFT BLANK

ATTACHMENT E
HUMAN RELIABILITY ANALYSIS

INTENTIONALLY LEFT BLANK

CONTENTS

	Page
ACRONYMS AND ABBREVIATIONS	E-11
E1 INTRODUCTION	E-13
E1.1 SUMMARY	E-13
E2 SCOPE AND BOUNDARY CONDITIONS	E-16
E2.1 SCOPE	E-16
E2.2 BOUNDARY CONDITIONS	E-16
E3 METHODOLOGY	E-18
E3.1 METHODOLOGY BASES	E-18
E3.2 GENERAL APPROACH	E-18
E3.2.1 Step 1: Define the Scope of the Analysis	E-18
E3.2.2 Step 2: Describe Base Case Scenarios	E-18
E3.2.3 Step 3: Identify and Define Human Failure Events of Concern	E-19
E3.2.3.1 Identifying Pre-initiator HFEs	E-20
E3.2.3.2 Identifying Human-Induced Initiator HFEs	E-20
E3.2.3.3 Identifying Non-recovery Post-initiator HFEs	E-20
E3.2.3.4 Identifying Recovery Post-initiator HFEs	E-20
E3.2.4 Step 4: Perform Preliminary Analysis and Identify HFEs for Detailed Analysis	E-21
E3.2.5 Step 5: Identify Potential Vulnerabilities	E-22
E3.2.6 Step 6: Search for HFE Scenarios	E-23
E3.2.7 Step 7: Quantify Probabilities of HFEs	E-23
E3.2.7.1 Qualitative Analysis	E-24
E3.2.7.2 Selection of Quantification Model	E-24
E3.2.7.3 Quantification	E-25
E3.2.7.4 Verification of Human Error Probabilities	E-25
E3.2.8 Step 8: Incorporate Human Failure Events into PCSA	E-26
E3.2.9 Step 9: Evaluation of HRA/PCSA Results and Iteration with Design	E-26
E3.3 DEPENDENCY	E-27
E3.3.1 Capturing Dependency	E-27
E3.3.2 Sources of Dependency	E-28
E3.4 UNCERTAINTY	E-28
E3.5 DOCUMENTATION OF RESULTS	E-29
E4 INFORMATION COLLECTION AND USE OF EXPERT JUDGMENT	E-30
E4.1 FACILITY FAMILIARIZATION AND INFORMATION COLLECTION	E-30
E4.1.1 General Information Sources	E-30
E4.1.2 Industry Data Reviewed by the HRA Team	E-32
E4.2 USE OF EXPERTS AND ENGINEERING JUDGMENT IN THE HRA	E-32
E4.2.1 Role of HRA Team Judgment	E-33
E4.2.1.1 HRA Team	E-34

CONTENTS (Continued)

	Page
E6.2.1.8	Cask Unbolting from Constraints and Movement from Cask Receipt Area to CTT E-61
E6.2.2	HFE Descriptions and Preliminary Analysis E-62
E6.2.3	Detailed Analysis E-67
E6.3	ANALYSIS OF HUMAN FAILURE EVENT GROUP #3: CASK PREPARATION AND MOVEMENT TO CASK UNLOADING ROOM E-67
E6.3.1	Group #3 Base Case Scenario E-68
E6.3.1.1	Initial Conditions and Design Considerations Affecting the Analysis E-68
E6.3.1.2	Preparation of HLW Cask for Transfer to Cask Unloading Room (HLW Only) E-69
E6.3.1.3	Preparation of Naval Cask for Transfer to Cask Unloading Room (Naval Cask Only) E-70
E6.3.1.4	Moving Transportation Cask on CTT into Cask Unloading Room (All Casks) E-73
E6.3.2	HFE Descriptions and Preliminary Analysis E-73
E6.3.3	Detailed Analysis E-81
E6.4	ANALYSIS OF HUMAN FAILURE EVENT GROUP #4: CTM ACTIVITIES: TRANSFER OF A CANISTER FROM A TRANSPORTAION CASK TO A WASTE PACKAGE WITH THE CTM E-81
E6.4.1	Group #4 Base Case Scenario E-81
E6.4.1.1	Initial Conditions and Design Considerations Affecting the Analysis E-82
E6.4.1.2	HLW Cask Lid Removal E-86
E6.4.1.3	Grapple Exchange and Installation E-87
E6.4.1.4	Canister Transfer to Waste Package E-87
E6.4.1.5	Naval Lift Adapter and Shield Ring Removal E-88
E6.4.1.6	Waste Package Preparation for Loading Room Departure ... E-88
E6.4.2	HFE Descriptions and Preliminary Analysis E-89
E6.4.3	Detailed Analysis for HFE Group #4 E-99
E6.4.3.1	Human Failure Events Requiring Detailed Analysis E-100
E6.4.3.2	Assessment of Potential Vulnerabilities (Step 5) E-100
E6.4.3.3	HFE Scenarios and Expected Human Failures (Step 6) E-103
E6.4.3.4	Quantitative Analysis (Step 7) E-106
E6.4.4	Results of Detailed HRA for HFE Group #4 E-149
E6.5	ANALYSIS OF HUMAN FAILURE EVENT GROUP #5: WASTE PACKAGE ASSEMBLY AND CLOSURE E-150
E6.5.1	Group #5 Base Case Scenario E-150
E6.5.1.1	Initial Conditions and Design Considerations Affecting the Analysis E-150
E6.5.1.2	Moving the WPTT with Loaded Waste Package under Waste Package Closure Room E-151

CONTENTS (Continued)

	Page
E6.5.1.3	Initiating Closure Process (Loaded Waste Package with HLW or Naval Waste) E-151
E6.5.1.4	Waste Package Welding E-151
E6.5.2	HFE Descriptions and Preliminary Analysis E-153
E6.5.3	Detailed Analysis E-157
E6.6	ANALYSIS OF HUMAN FAILURE EVENT GROUP #6: WASTE PACKAGE EXPORT E-157
E6.6.1	Group #6 Base Case Scenario E-157
E6.6.1.1	Initial Conditions and Design Considerations Affecting the Analysis E-157
E6.6.1.2	Loaded and Sealed Waste Package Movement to Waste Package Loadout Room and WPTT Docking Station Engagement E-158
E6.6.1.3	Waste Package Shield Ring Removal and Movement of Shield Ring to Waste Package Shield Ring Stand E-158
E6.6.1.4	WPTT Horizontal Rotation E-158
E6.6.1.5	Waste Package Inspection and Loading into TEV E-159
E6.6.2	HFE Descriptions and Preliminary Analysis E-159
E6.6.3	Detailed Analysis for HFE Group #6 E-165
E6.6.3.1	Human Failure Events Requiring Detailed Analysis E-166
E6.6.3.2	Assessment of Potential Vulnerabilities (Step 5) E-166
E6.6.3.3	HFE Scenarios and Expected Human Failures (Step 6) E-170
E6.6.3.4	Quantitative Analysis (Step 7) E-171
E6.6.4	Results of Detailed HRA for HFE Group #6 E-178
E7	RESULTS: HUMAN RELIABILITY ANALYSIS DATABASE E-179
E8	REFERENCES E-183
E8.1	DESIGN INPUTS E-183
E8.2	DESIGN CONSTRAINTS E-185
APPENDIX E.I	RECOMMENDED INCORPORATION OF HUMAN FAILURE EVENTS IN THE YMP PCSA E-186
APPENDIX E.II	GENERAL STRUCTURE OF POST-INITIATOR HUMAN ACTIONS E-187
APPENDIX E.III	PRELIMINARY (Screening) Quantification PROCESS for Human Failure Events E-188
APPENDIX E.IV	SELECTION OF METHODS FOR DETAILED QUANTIFICATION E-193
APPENDIX E.V	HUMAN FAILURE EVENTS NAMING CONVENTION E-197

FIGURES

	Page
E6.0-1. HFE Groups Associated with Facility Operations.....	E-43
E6.1-1. Activities Associated with HFE Group #1.....	E-49
E6.2-1. Activities Associated with HFE Group #2.....	E-55
E6.3-1. Activities Associated with HFE Group #3.....	E-67
E6.4-1. Activities Associated with HFE Group #4.....	E-81
E6.4-2. Canister Transfer Machine—Side View.....	E-85
E6.4-3. Canister Transfer Machine—End View.....	E-86
E6.5-1. Activities Associated with HFE Group #5.....	E-150
E6.6-1. Activities Associated with HFE Group #6.....	E-157
E6.6-2. Waste Package Positioning Room and Waste Package Loadout Room Conceptual Configuration.....	E-169
E.I-1. Modeling Strategy for HFE Types.....	E-186
E.II-1. Post Initiator Operator Action Event Tree.....	E-187
E.V-1. Basic Event Naming Convention.....	E-197

INTENTIONALLY LEFT BLANK

TABLES

	Page
E3.2-1. Human Performance Limiting Values	E-26
E3.3-1. Formulae for Addressing HFE Dependencies	E-28
E3.4-1. Lognormal Error Factor Values	E-29
E6.0-1. Correlation of HFE Groups to ESDs and HAZOP Evaluation (PFD) Nodes.....	E-45
E6.0-2. Summary of Preliminary Values for the Cross-group Generic HFEs.....	E-49
E6.1-1. HFE Group #1 Descriptions and Preliminary Analysis.....	E-53
E6.2-1. HFE Group #2 Descriptions and Preliminary Analysis.....	E-63
E6.3-1. HFE Group #3 Descriptions and Preliminary Analysis.....	E-75
E6.4-1. HFE Group #4 Descriptions and Preliminary Analysis.....	E-91
E6.4-2. Group #4 HFEs Requiring Detailed Analysis.....	E-100
E6.4-3. HFE Scenarios and Expected Human Failures for Group #4	E-104
E6.4-4. HEP Model for Group #4 Scenario 1(a) for 51A-OpCTMdrop001-HFI-COD	E-111
E6.4-5. HEP Model for Group #4 Scenario 1(b) for 51A-OpCTMdrop001-HFI-COD.....	E-113
E6.4-6. HEP Model for Group #4 Scenario 1(c) for 51A-OpCTMdrop001-HFI-COD.....	E-117
E6.4-7. HEP Model for Group #4 Scenario 1(d) for 51A-OpCTMdrop001-HFI-COD.....	E-121
E6.4-8. HEP Model for Group #4 Scenario 1(e) for 51A-OpCTMdrop001-HFI-COD.....	E-122
E6.4-9. HEP Model for HFE Group #4 Scenario 2(a) for 51A-OpCTMdrop002-HFI-COD	E-126
E6.4-10. HEP Model for HFE Group #4 Scenario 2(b) for 51A-OpCTMdrop002-HFI-COD	E-128
E6.4-11. HEP Model for HFE Group #4 Scenario 2(c) for 51A-OpCTMdrop002-HFI-COD	E-132
E6.4-12. HEP Model for HFE Group #4 Scenario 2(d) for 51A-OpCTMdrop002-HFI-COD	E-135
E6.4-13. HEP Model for HFE Group #5 Scenario 3(a) for 51A-OpCTMImpact1-HFI-COD	E-139
E6.4-14. HEP Model for HFE Group #5 Scenario 3(b) for 51A-OpCTMImpact1-HFI-COD	E-143
E6.4-15. HEP Model for HFE Group #5 Scenario 3(c) for 51A-OpCTMImpact1-HFI-COD	E-146
E6.4-16. HEP Model for HFE Group #5 Scenario 3(d) for 51A-OpCTMImpact1-HFI-COD	E-149

TABLES (Continued)

	Page
E6.4-17. Summary of HFE Detailed Analysis for HFE Group #4	E-150
E6.5-1. HFE Group #5 Descriptions and Preliminary Analysis	E-155
E6.6-1. HFE Group #6 Descriptions and Preliminary Analysis	E-161
E6.6-2. Group #6 HFE Requiring Detailed Analysis	E-166
E6.6-3. HFE Scenarios and Expected Human Failures for Group #6	E-170
E6.6-4. HEP Model for HFE Group #6 Scenario 1(a) for 51A-OpDirExpose3-HFI- NOD	E-175
E6.6-5. HEP Model for HFE Group #6 Scenario 1(b) for 51A-OpDirExpose3-HFI- NOD	E-176
E6.6-6. HEP Model for HFE Group #6 Scenario 1(c) for 51A-OpDirExpose3-HFI- NOD	E-178
E6.6-7. Summary of HFE Detailed Analysis for HFE Group #6	E-178
E7-1. HFE Data Summary	E-179
E.III-1. Examples of Information Useful to HFE Quantification	E-188
E.III-2. Types of HFES	E-191
E.IV-1. Comparison between NPP and YMP Operations	E-193
E.V-1. Human Failure Event Type Codes and Failure Mode Codes	E-198

ACRONYMS AND ABBREVIATIONS

Acronyms

APOA	assessed proportion of affect
ASD	adjustable speed drive
ASME	American Society of Mechanical Engineers
ATHEANA	A Technique for Human Event Analysis
BSC	Bechtel SAIC Company, LLC
CFF	cognitive function failure
CPC	common performance condition
CREAM	Cognitive Reliability and Error Analysis Method
CTM	canister transfer machine
CTT	cask transfer trolley
DOE	U.S. Department of Energy
EFC	error forcing context
EOC	error of commission
EOO	error of omission
EPC	error-producing condition
EPRI	Electric Power Research Institute
ESD	event sequence diagram
GTT	generic task type
HAZOP	hazard and operability
HCR	Human Cognitive Reliability
HEART	Human Error Assessment and Reduction Technique
HEP	human error probability
HFE	human failure event
HLW	high-level radioactive waste
HRA	human reliability analysis
HVAC	heating, ventilation, and air conditioning
IHF	Initial Handling Facility
INPO	Institute of Nuclear Power Operations
ISFSI	independent spent fuel storage installation
ITS	important to safety
LIS	Licensing Information Service
MAP	mobile access platform
MLD	master logic diagram
NARA	Nuclear Action Reliability Assessment

ACRONYMS AND ABBREVIATIONS (Continued)

NASA	National Aeronautics and Space Administration
NDE	nondestructive examination
NPP	nuclear power plant
NRC	U.S. Nuclear Regulatory Commission
ORE	Operator Reliability Experiments
PCSA	preclosure safety analysis
PFD	process flow diagram
PIC	person in charge
PLC	programmable logic controller
PRA	probabilistic risk assessment
PSF	performance-shaping factor
RHS	remote handling system
SHARP	Systematic Human Action Reliability Procedure
SPAR-H	Standardized Plant Analysis Risk Human Reliability Analysis
SPM	site prime mover
SSCs	structures, systems, and components
TEV	transport and emplacement vehicle
THERP	Technique for Human Error Rate Prediction
TRC	Time-Reliability Correlations
UT/ET	ultrasonic testing/eddy current testing
WPTT	waste package transfer trolley
YMP	Yucca Mountain Project

Abbreviations

in. inch

E1 INTRODUCTION

This document describes the work scope, definitions, terms, methods, and analysis for the human reliability analysis (HRA) task of the Yucca Mountain Project (YMP) preclosure safety analysis (PCSA) reliability assessment.

The HRA task identifies, models, and quantifies human failure events (HFEs) postulated in the PCSA to assess the impact of human actions on event sequences modeled in the PCSA. The HFEs evaluated and quantified by this task are identified during the following activities:

- Initiating event identification and grouping
- Event sequence development and categorization
- System analysis
- Sequence quantification and uncertainty analysis.

The HRA task ensures that the HFEs identified by the other tasks (e.g., hazard and operability (HAZOP) evaluation, event sequence diagram (ESD) development, event tree analysis, fault tree analysis) are quantified with HRA techniques. The ESD finding is that the human-induced initiating events dominate the HRA. No post-initiator human actions have been credited in this analysis. The HRA task also ensures that modeled HFEs are appropriately incorporated into the PCSA and provides appropriate human error probabilities (HEPs) for all modeled HFEs. It is important to note that YMP operations differ from those of traditional nuclear power plants (NPPs), and the HRA analysis reflects these differences; Appendix E.IV of this analysis provides further discussion on these differences and how they influenced the choice of methodology.

E1.1 SUMMARY

The HRA was carried out using a nine-step process that is derived from *A Technique for Human Event Analysis (ATHEANA)* (Ref. E8.1.22):

1. Define the scope of the analysis.
2. Describe the base case progression of actions and responses that constitute successful completion of the operations being evaluated (base case scenarios).
3. Identify and define HFEs of concern.
4. Perform preliminary (screening) analysis and identify HFEs requiring detailed analysis.
5. Identify potential vulnerabilities for the HFEs requiring detailed analysis.
6. Search for HFE scenarios (i.e., scenarios of concern).
7. Quantify probabilities of HFEs.

8. Incorporate HFEs into the PCSA.
9. Evaluate HRA/PCSA results and iterate with design.

After the scope was defined, the facility operations were split into logical groups that relate to the various phases of the Initial Handling Facility (IHF) operations. For each of these operational phase groups, a base case scenario was defined that describes in detail the normal operations for that group. Once the operations were defined and the base cases were documented, HFEs were identified through an iterative process whereby the human reliability analysts, in conjunction other PCSA analysts and Engineering and Operations personnel, met and discussed the design and operations in order to appropriately model the human interface. This process consisted of the HAZOP evaluation, master logic diagram (MLD) and event sequence development, fault tree and event tree modeling, and it culminated in the preliminary analysis and incorporation of HFEs into the model. The iteration with the event sequence and system reliability analysis also identified HFEs of potential concern. HFEs identified include both errors of omission (EOOs) and errors of commission (EOCs).

Included in this process was an extensive information collection process where the human reliability analysts reviewed industry data and interviewed subject matter experts to identify potential vulnerabilities and HFE scenarios.

The result of this identification process was a list of HFEs and a description of each HFE scenario, including system and equipment conditions and any resident or triggered human factor concerns (e.g., performance-shaping factors (PSFs)). This combination of conditions and human factor concerns then became the error forcing context (EFC) for a specific HFE. Additions and refinements to these initial EFCs were made during the preliminary and detailed analyses.

A preliminary, or screening-type, analysis was then performed to preserve HRA resources so that detailed analyses can be focused on only the most risk-significant HFEs. The preliminary analysis included verification of the validity of HFEs included in the initial PCSA model, assignment of a conservative screening value (mean value) to each HFE, and verification of preliminary values. The actual quantification of preliminary values was a six-step process that is described in detail in Appendix E.III of this analysis. Once the preliminary values were assigned, the PCSA model was quantified (initial quantification), and HFEs were identified for detailed analysis if: (1) the HFE was a risk-driver for a dominant sequence, and (2) using the preliminary values, that event sequence was above Category 1 or 2 according to the 10 CFR Part 63 (Ref. E8.2.1) performance objectives. The remaining HFEs retained their preliminary values. While most of the activities associated with preliminary analysis were time-consuming, extra care was taken to perform these tasks conscientiously since the results of the initial quantification were used to identify which HFEs require detailed analysis.

Although many of the HFEs are modeled in a simplified form in the event trees and fault trees for the preliminary analysis, each action is separated as much as possible for the detailed analysis. This separation is done to ensure that the detailed analysis is thorough and that the relationship between the system functionality and operations crew is transparent. First an HFE is broken down into the various scenarios that lead to the failure. Then, each scenario is further broken down into specific required actions and their applicable procedures, along with the

systems and components that must be operated during performance of each action. Each action in each scenario has its own unique context, dependencies, and set of PSFs, and each was thus quantified independently. The failure probabilities for these unsafe actions were quantified by the HRA method appropriate to the HFE, its classification (e.g., EOC, EOO, observation error, execution error), and the context. The HRA methods used in this analysis include the Technique for Human Error Prediction (THERP) (Ref. E8.1.26), Human Error Assessment and Reduction Technique (HEART) (Ref. E8.1.28), Nuclear Action Reliability Assessment (NARA) (Ref. E8.1.11), Cognitive Reliability and Error Analysis Method (CREAM) (Ref. E8.1.18), and the expert elicitation process from ATHEANA (Ref. E8.1.22).

As described in Appendix E.IV of this analysis, no single HEP quantification method is suitable for all HFEs identified in the event sequence quantification. For example, there are unsafe actions within the YMP HFEs that would best fit the HEART (Ref. E8.1.28)/NARA (Ref. E8.1.11) approach and others that would best fit the CREAM (Ref. E8.1.18) approach. The documentation of each HFE subjected to a detailed analysis defines the method used and the basis for its use.

After estimates for HFE probabilities were generated, these results were reviewed by the human reliability team and, in some cases, by knowledgeable operations personnel as a “sanity check.” Principally, such checks were used, for example, to compare the probabilities of different HFEs and determine whether or not these probabilities were reasonable. A review of this type was particularly important for HFE probabilities that were generated using data from the THERP method (Ref. E8.1.26) because THERP does not account for PSFs in a standard formulaic way. In addition, the HFE probability estimates were reviewed to ensure that they did not exceed the lower limit of credible human performance as defined by NARA (Ref. E8.1.11). For the preliminary analysis, HFEs were modeled at a high level in order to reduce dependencies that arise from modeling detailed actions. For a detailed assessment, where the various actions that constitute an HFE were explicitly quantified, dependencies were also explicitly addressed using the method described in THERP (Ref. E8.1.26), which is adopted by NARA (Ref. E8.1.11)

HFE probabilities produced in this analysis are mean values with associated error factors. Uncertainties in both the preliminary and detailed HEP quantification were accounted for by assigning a lognormal distribution and applying an error factor of 3, 5, or 10 to the distribution, depending on the mean value of the final HEP.

Because the YMP design and operations were still evolving during the course of this analysis, they could be changed in response to the analysis. This iteration was particularly necessary when an event sequence proved to be noncompliant with the performance objectives of 10 CFR Part 63 (Ref. E8.2.1) because the probability of a given HFE dominated the probability of that event sequence. In those cases, a design feature or procedural control was added to reduce the probability or completely eliminate the HFE, and the scenario was reanalyzed for human failures.

To guide the reader through the analysis, Section E6.0.1 explains how the HRA write-up is structured and how it interfaces with other parts of the PCSA, including a simplified diagram of the facility operations (which defines analysis sections) and a map that links this analysis back to the MLD, the ESD, and the HAZOP evaluation.

E2 SCOPE AND BOUNDARY CONDITIONS

E2.1 SCOPE

The scope of the HRA is established in order to focus the analysis on the issues pertinent to the goals of the overall PCSA. Thus, the scope is as follows:

1. HFEs are only considered if they contribute to a scenario that has the potential to result in a release of radioactivity, a criticality event, or a radiation exposure to workers.
2. Pursuant to the above, the following types of HFEs are excluded:
 - A. HFEs resulting in standard industrial injuries (e.g., falls)
 - B. HFEs resulting in the release of hazardous nonradioactive materials, regardless of amount
 - C. HFEs resulting solely in delays to or losses of process availability, capacity, or efficiency.
3. The identification of HFEs is restricted to those areas of the facility that handle waste forms and only during the times that waste forms are being handled (e.g., HFEs are not identified for the Cask Preparation Room during export of empty transportation casks).
4. The exception to #3 is that system-level HFEs are considered for support systems when those HFEs could result in a loss of a safety function related to the occurrence or consequences associated with the events specified in #1.
5. Recovery post-initiator actions (as defined in Section E5.1.1.1) are not credited in the analysis; therefore, HFEs associated with them are not considered.
6. In accordance with Section 4.3.10.1 (boundary conditions of the PCSA), initiating events associated with conditions introduced in structures, systems, and components (SSCs) before they reach the site are not, by definition of 10 CFR 63.2 (Ref. E8.2.1), within the scope of the PCSA nor, by extension, within the scope of the HRA.

E2.2 BOUNDARY CONDITIONS

Unless specifically stated otherwise, the following general conditions and limitations are applied throughout the HRA task. The first two conditions are absolute. The remaining conditions apply unless there is reason to believe that they do not apply. The analyst determines whether those conditions apply for each individual action considered.

- Only HFEs made in the performance of assigned tasks are considered. Malevolent behavior (i.e., deliberate acts of sabotage and the like) are not considered in this task.
- All facility personnel act in a manner they believe to be in the best interests of the plant. Any intentional deviation from standard operating procedures is made because

employees believe their actions to be more efficient or because they believe the action as stated in the procedure to be unnecessary.

- Since the YMP is currently in the design phase, facility-specific information and operating experience is generally not available. The only available substitute is similar operations involving similar hazards and equipment. Examples would include spent nuclear fuel (SNF) handling at reactor sites having independent spent fuel storage installations (ISFSIs), chemical munitions handling at U.S. Army chemical demilitarization facilities, and any other facilities whose primary function includes handling and disposal of very large containers of extremely hazardous material. Equipment design and operational characteristics at the geologic repository operations area facilities once they are built and operating (including crew structures, training, and interactions) are adequately represented by these currently operating facilities.
- The facility is initially operating under normal conditions and is designed to the highest quality human factors specifications. The level of operator stress is optimal unless otherwise noted in the analysis.
- In performing the operations, the operator does not need to wear protective clothing unless the operation is similar to those performed in other comparable facilities where protective clothing is required.
- The tasks are performed by qualified personnel, such as operators, maintenance workers, or technicians. All personnel are certified in accordance with the training and certification program stipulated in the license. They are experienced and have functioned in their present positions for a sufficient amount of time to be proficient.
- The environment in the facility is not adverse. The levels of illumination and sound and the provisions for physical comfort are optimal. Judgment is required to determine what constitutes optimal environmental conditions. The analyst makes this determination and, as part of the assessment of performance, documents influencing factors when there is a belief that the action is likely to take place in a suboptimal environment.
- Personnel involved with the facility operations are expected to have the proper training commensurate with nuclear industry standards. As appropriate, this training is followed by a period of observation until the operator is proficient.
- While all personnel are trained to procedures, and procedures exist for all work required, the direct presence and use of procedures (including checklists) during operation is generally restricted to actions performed in the control room. Workers performing skill-of-craft operations do not carry written procedures on their person while performing their activities.

These factors are evaluated qualitatively for each situation being analyzed.

E3 METHODOLOGY

E3.1 METHODOLOGY BASES

The HRA task is performed in a manner that implements the intent of the high-level requirements for HRA in the American Society of Mechanical Engineers (ASME RA-S-2002 *Standard for Probabilistic Risk Assessment for Nuclear Power Plant Applications* (Ref. E8.1.4) and incorporates the guidance provided by the U.S. Nuclear Regulatory Commission (NRC) in *Preclosure Safety Analysis – Human Reliability Analysis* (Ref. E8.1.23).

E3.2 GENERAL APPROACH

The HRA consists of several steps that follow the intent of ASME RA-S-2002 (Ref. E8.1.4) and the process guidance provided in *Technical Basis and Implementation Guidelines for a Technique for Human Event Analysis (ATHEANA)*, NUREG-1624 (Ref. E8.1.22). Detailed descriptions of each HRA step are provided in the following subsections to summarize the processes used by the analysts. The step descriptions are based on the ATHEANA documentation, with some passages taken essentially verbatim and others paraphrased to adapt the material based on NPPs to the YMP facilities. Additional information is available in the ATHEANA documentation (Ref. E8.1.22). Further discussion on information collection and use of expert judgment in this process can be found in Section E4.

HFE probabilities produced in this analysis are mean values. The HEPs are modeled as a lognormal distribution, where the error factors are defined based on the method presented in Section E3.4.

E3.2.1 Step 1: Define the Scope of the Analysis

The objective of the YMP HRA is to provide a comprehensive quantitative assessment of the HFES that can contribute to the facility's event sequences resulting in radiological release, criticality, or direct exposure. Any aspects of the work that provide a basis for bounding the analysis are identified in this step. In the case of the YMP, the scope is bounded by the design state of the facilities and equipment.

E3.2.2 Step 2: Describe Base Case Scenarios

In this step, the base case scenarios are defined and characterized for the operations being evaluated. In general, there is one base case scenario for each operation included in the model. The base case scenario:

- Represents the most realistic description of expected facility, equipment, and operator behavior for the selected operation.
- Provides a basis from which to identify and define deviations from such expectations (Step 6).

In the ideal situation (which is seldom achieved), the base case scenario:

- Has a consensus operator model¹
- Is well-defined operationally
- Has well-defined physics
- Is well-documented in public or proprietary references
- Is realistic.

Since operators and “as built, as operated” information are not currently available for YMP, this information is sought from comparable facilities with comparable operations. Documented reference analyses (e.g., engineering analyses) can assist in defining the scenario from the standpoint of physics and operations. The reference analyses may need to be modified to be more realistic. Expert judgment, engineering documents and applicable industry experience are the keys to defining realistic base case scenarios for YMP operations; Section E4 provides greater detail on how information was collected and the role of subject matter experts in this process.

E3.2.3 Step 3: Identify and Define Human Failure Events of Concern

Possible HFEs and/or unsafe actions (i.e., actions inappropriately taken, or actions not taken when needed) that result in a degraded state are generally identified and defined in this step. After HFEs are identified they must be classified to support subsequent steps in the process. The classification process is described further in Section E5.1.1. The analyses performed in later steps (i.e., Steps 4 through 7) may identify the need to define an HFE or unsafe action not previously identified in Step 3.

Human errors were identified based upon the three temporal parts generally analyzed by probabilistic risk assessment (PRA) and are categorized as follows:

- Pre-initiator HFEs
- Human-induced initiator HFEs
- Post-initiator HFEs²:
 - Non-recovery
 - Recovery.

Each of these types of HFEs is defined in Section E5.1.1.1; identification of the HFEs for each temporal phase is described in the following sections.

The result of this identification process is a list of HFEs and a description of each HFE scenario, including system and equipment conditions and any resident or triggered human factor concerns

¹ATHEANA (Ref. E8.1.22), Section 9.3.1 defines a consensus operator model in the following manner: “Operators develop mental models of plant responses to various PRA initiating events through training and experience. If a scenario is well defined and consistently understood among all operators (i.e., there is a consensus among the operators), then there is a consensus operator model.”

²Terminology common to NPPs refer to non-recovery post-initiator events as Type C events and recovery events as Type CR events.

(e.g., PSFs). This combination of conditions and human factor concerns then becomes the EFC for a specific HFE. Additions to and refinements of these initial EFCs are made during the preliminary and detailed analyses.

E3.2.3.1 Identifying Pre-initiator HFEs

Pre-initiators are identified by the system analysts when modeling fault trees, while performing the system analysis task. Special attention is paid to the possibility that an error can be repeated in similar redundant components or trains, leading to a human common-cause failure.

E3.2.3.2 Identifying Human-Induced Initiator HFEs

Human-induced initiator HFEs are identified through an iterative process whereby the human reliability analysts, in conjunction with other PCSA analysts and engineering and operations personnel, meet and discuss the design and operations of the facility and SSCs in order to appropriately model the human interface. This iterative process begins with the HAZOP evaluation and MLD, described and documented in *Initial Handling Facility Event Sequence Development Analysis* (Ref. E8.1.10), followed by a second iteration during the initial fault tree and event tree modeling, and ending with a third iteration through the preliminary analysis and incorporation of HFEs into the model. Included in this process is an extensive information collection process where industry data was reviewed (Section E4.1) and subject matter experts were interviewed (Section E4.2) to identify potential vulnerabilities and HFE scenarios. HFEs identified include both EOOs and EOCs.

E3.2.3.3 Identifying Non-recovery Post-initiator HFEs

Non-recovery post-initiator HFEs are identified by examining the human contribution to pivotal events in the event tree analysis. The event sequence analysts, with support from the human reliability analysts, identify HFEs that represent the operator's failure to perform the proper action to mitigate the initiating event and/or the unavailability of automatic mitigation functions as called for in the emergency operating procedures or in accordance with their emergency response training. This identification includes all actions required, whether in a control room or locally. Post-initiator EOCs and EOOs are also considered. It should be emphasized that this section presents the methodology that is used to identify non-recovery post-initiator events. However, as shown in Section E6, none of these types of errors have been identified for the IHF event sequence and categorization analysis. During the qualitative evaluation, non-recovery post-initiator events were considered and ruled out because it was unnecessary to credit non-recovery actions to demonstrate compliance with the performance objectives stated in 10 CFR 63.111 (Ref. E8.2.1).

E3.2.3.4 Identifying Recovery Post-initiator HFEs

Recovery actions are of limited relevance to YMP operations and, for conservatism, were not credited in this analysis. Recovery post-initiator HFEs are outside the scope of this analysis (Section E2.1).